Molecular Catalysis 456 (2018) 75–86

Contents lists available at ScienceDirect

Molecular Catalysis

journal homepage: www.elsevier.com/locate/mcat

Osmium(II)/R-pybox *vs* ruthenium(II)/R-pybox complexes in the catalytic asymmetric transfer hydrogenation of arylketones

Eire de Julián, Nuria Fernández, Josefina Díez, Elena Lastra, M. Pilar Gamasa*

Departamento de Química Orgánica e Inorgánica-IUQOEM (Unidad Asociada al CSIC), Centro de Innovación en Química Avanzada (ORFEO-CINQA), Universidad de Oviedo, 33006 Oviedo, Principado de Asturias, Spain

ARTICLE INFO

Keywords:
Asymmetric transfer hydrogenation of ketones
Osmium
Ruthenium
Enantiopure pybox
Nitrogen-donor ligands

ABSTRACT

The reaction of the complexes *trans*-[$RuCl_2(\eta^2\text{-}C_2H_4)$\{(*S*,*S*)-^{i}Pr-pybox\}] (**1a**) and *trans*-[$RuCl_2(\eta^2\text{-}C_2H_4)$\{(*R*,*R*)-Ph-pybox\}] (**1b**) with nitrogen heterocyclic ligands, provide the complexes *trans*-[$RuCl_2$(L)(R-pybox)] (L = py (**3a,b**), 3-Br-py (**4a,b**), isoquinoline (**5a,b**), pyrazine (**6a,b**), 1-methylimidazole (**7a,b**), 1-benzylimidazole (**8a,b**), pyrazole (**9a,b**), 3-methylpyrazole (**10a,b**), and 1H-1,2,4-triazole (**11a,b**)). The complexes *trans*-[$OsCl_2$(L)\{(*S*,*S*)-^{i}Pr-pybox\}] (L = py (**12**), 3-Br-py (**13**), 3-CN-py (**14**), 3-MeO-py (**15**), 3-NO_2-py (**16**), 4-CN-py (**17**), 4-MeO-py (**18**), isoquinoline (**19**), 1-methylimidazole (**20**), 1-benzylimidazole (**21**), pyrazole (**22**)) have been similarly synthesized by the substitution of ethylene from the precursor complex *trans*-[$OsCl_2(\eta^2\text{-}C_2H_4)$\{(*S*,*S*)-^{i}Pr-pybox\}] (**2**) by the corresponding N-donor ligand in refluxing toluene. Moreover, the dinuclear complexes [$(RuCl_2$\{(*S*,*S*)-^{i}Pr-pybox\}$)_2(\mu\text{-}N,N\text{-}C_4H_4N_2)$] (**23a**), [$(RuCl_2$\{(*R*,*R*)-Ph-pybox\}$)_2(\mu\text{-}N,N\text{-}C_4H_4N_2)$] (**23b**) and [$(OsCl_2$\{(*S*,*S*)-^{i}Pr-pybox\}$)_2(\mu\text{-}N,N\text{-}C_4H_4N_2)$] (**24**) have been prepared by the reaction of the complexes **1** and **2** with pyrazine (1:0.5 M ratio for **23** and 1:1.5 for **24**). The structure of the complexes **9a**, **12**, **23a** and **24** has been determined by single-crystal X-ray diffraction analysis. The ruthenium **3a,b**, **6a** and **10a,b** and osmium complexes **12–22** and **24** have been assayed as catalysts for the asymmetric transfer hydrogenation reaction. Among them, the osmium complexes **12**, **15**, **16**, **18** and **24** have proven more efficient in the reduction of a variety of aromatic ketones affording the (*R*)-benzylalcohols with very high conversion and moderate enantioselectivity up to 73% *e.e.*

1. Introduction

The asymmetric transfer hydrogenation (ATH) of prochiral ketones leading to enantiopure alcohols has been usually focused on the use of ruthenium, rhodium and iridium catalysts containing well designed chiral ligands [1], although other late transition metal complexes have also been also studied [2]. In spite that osmium catalysts have been traditionally considered less active than the ruthenium analogs due to their slower ligand exchange kinetics and, consequently, only occasionally employed [3], the Baratta's group [4] has demonstrated in the last years that osmium complexes containing Josiphos-type phosphanes [5], and substituted aminomethylpyridines show great potential in this field displaying comparable catalytic activity as related ruthenium complexes. Specifically, the complexes *in situ* generated from [$OsCl_2(PPh_3)_3$], (*S*,*R*)-Josiphos or (*S*,*R*)-Josiphos* and (pyridin-2-yl)alkanamine derivatives (R-Pyme and H-Pyme) (Chart 1, ligands A) promoted the ATH of acetophenone and methyl-arylketones to the corresponding *S*-alcohols with high TOF (up to 1.9×10^4 h^{-1}) and *e.e.* (91–96%) [6]. These results are rather similar to those reached using the corresponding ruthenium complexes [7]. This group also studied the catalytic potential of ruthenium and osmium complexes [MCl(CNN)(PP)] containing Josiphos-type ligands and anionic CNN pincer ligands derived from 1-(6-arylpyridin-2-yl)alkanamine (Chart 1, ligands B–D) [8–10], and (benzo[*h*]quinolin-2-yl)alkanamine (Chart 1, ligands E) [11]. They found that both types of metal complexes behave very efficiently for transfer hydrogenation of methylarylketones (Ru: TOF up to 1.3×10^6 h^{-1}, 81–99% *e.e.*; Os: TOF up to 4.0×10^5 h^{-1}, 91–97% *e.e.*) [8–11]. Interestingly, the nature of the enantiopure pyridine-derived and Josiphos-type ligands notably improved the reduction efficiency. In fact, the isolated complexes [MCl(CNN)\{(*R*,*S*)-Josiphos*\}] (M = Ru, Os; HCNN = (*S*)-1-(6-(2-naphtyl)pyridin-2-yl)ethanamine (Chart 1, ligand D(r)) provided the best results, in terms of rate (TOF 10^5-10^6 h^{-1}) and enantioselectivity (up to 99% *e.e.*), for the conversion of different alkylaryl ketones and methylpyridyl ketones into the corresponding alcohols [10].

In this context we have recently reported on the capability of the

* Corresponding author.
E-mail address: pgb@uniovi.es (M.P. Gamasa).

https://doi.org/10.1016/j.mcat.2018.07.002
Received 3 May 2018; Received in revised form 1 July 2018; Accepted 3 July 2018

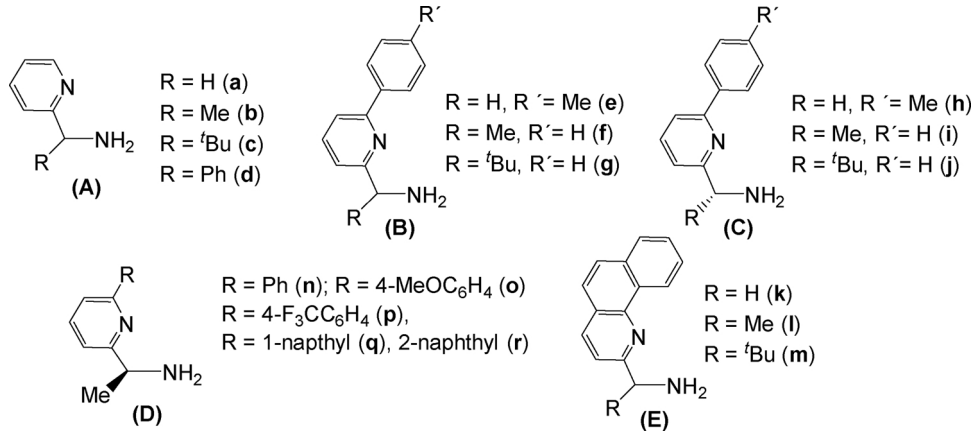

Chart 1. (pyridine-2-yl)alkanamine, 1-[6-arylpyridin-2-yl)alkanamine and (benzo[*h*]quinolin-2-yl)alkanamine ligands.

osmium and ruthenium complexes *cis*-[$RuCl_2$(L){(*R*,*R*)-Ph-pybox}] (L = PPh_3, P^iPr_3) [12] and *trans*-[$OsCl_2$(L){(*S*,*S*)-^{i}Pr-pybox)] (L = P$(OR)_3$) [13] towards the asymmetric transfer hydrogenation of aryl ketones. In all cases, both catalysts behave similarly affording more than 95% of conversion and up to 95% of *e.e.* Moreover, it constitutes the first application of an osmium catalyst bearing an aprotic nitrogen ligand as the chiral asymmetric inductor in the ATH of ketones. On the other hand, it was found that the nature of the achiral ligand has notable influence on the efficiency of these catalysts [12,13]. After these promising results, it seems therefore apparent to undertake further studies by choosing ligands with electronic/steric demand properties different than those of the mentioned phosphorous ligands.

Accordingly, we report herein the synthesis of new ruthenium *trans*-[$RuCl_2$(L)(R-pybox)] (R-pybox = (*S*,*S*)-^{i}Pr-pybox, (*R*,*R*)-Ph-pybox)) and osmium complexes *trans*-[$OsCl_2$(L){(*S*,*S*)-^{i}Pr-pybox}] containing achiral N-donor ligands, specifically five- and six-membered aromatic nitrogen heterocycles, which feature very different electronic properties than the P-donor ligands (phosphanes and phosphites) already reported. Moreover, the catalytic activity of some of these complexes towards the AHT of ketones is explored.

2. Results and discussion

*2.1. Synthesis of the complexes trans-[$RuCl_2$(L)(R-pybox)] [R-pybox = (S,S)-^{i}Pr-pybox = 2,6-bis[4'-(S)-isopropyloxazolin-2´-yl]pyridine, L = py (**3a**), 3-Br-py (**4a**), isoquinoline (**5a**), pyrazine (**6a**); R-pybox = (R,R)-Ph-pybox = 2,6-bis[4'-(R)-phenyloxazolin-2´-yl]pyridine, L = py (**3b**), 3-Br-py (**4b**), isoquinoline (**5b**), pyrazine (**6b**)]*

We have firstly carried out the preparation of ruthenium complexes wherein the metal is coordinated to six-membered nitrogen heterocycles, *e.g.* pyridine, isoquinoline, and pyrazine (complexes **3**,**4**,**5**,**6**, respectively). Thus, the complexes *trans*-[$RuCl_2$(η^2-C_2H_4)(R-pybox)] **1** (**1a**: R^1 = ^{i}Pr, R^2 = H; **1b**: R^1 = H, R^2 = Ph**)** were reacted with the *N*-donor ligands pyridine, 3-Br-pyridine, isoquinoline and pyrazine in dichloromethane (**1a**: reflux, 1:1.5 M ratio; **1b**: 60 °C, sealed tube, 1:2 M ratio) giving rise stereoselectively to the formation of the *trans*-complexes **3–6** in moderate to very high yield (**3a**-**6a**: 87–98 %; **3b**-**6b**: 58–81%) by ethylene/*N*-donor ligand exchange (Scheme 1; see Experimental Section for details).

The *trans* stereochemistry of the complexes **3–6** has been readily determined on the basis of the ^{1}H and ^{13}C{^{1}H} NMR spectra that are fully consistent with the presence of a C_2 symmetry axis. Thus, the ^{13}C{^{1}H} NMR spectra of the complexes **3–6** show single resonance signals for the C-2´ (OCN), C-4´ (CHR) and C-5´ (CH_2) carbon atoms of both pybox-oxazoline rings and for the C-3/C-5 and C-2/C-6 carbon atoms of the pybox pyridine ring.

*2.2. Synthesis of the complexes trans-[$RuCl_2$(L)(R-pybox)] [R-pybox = (S,S)-^{i}Pr-pybox, L = 1-methylimidazole (**7a**), 1-benzylimidazole (**8a**), pyrazole (**9a**), 3-methylpyrazole (**10a**), and 1H-1,2,4-triazole (**11a**); R-pybox = (R,R)-Ph-pybox, L = 1-methylimidazole (**7b**), 1-benzylimidazole (**8b**), pyrazole (**9b**), 3-methylpyrazole (**10b**), and 1H-1,2,4-triazole (**11b**)]*

Under the same reaction conditions as described above, the corresponding ruthenium complexes having an azole ligand were then synthesized from complexes **1a**,**b** and 1-methyl and 1-benzylimidazole (**7**,**8**; 66–93% yield), pyrazole and 3-methylpyrazole (**9**,**10**; 76–97% yield) and 1*H*-1,2,4-triazole (**11**; 83–95% yield) (Scheme 2; see Experimental Section for details). The *trans* arrangement of the chlorine atoms was also confirmed by the presence of a C_2 symmetry axis (see the ^{1}H and ^{13}C{^{1}H} NMR spectra).

The structure of the complex **9a** has been confirmed by a single crystal X-ray analysis. The asymmetric unit of the complex **9a** consists of two molecules that have similar relevant structural parameters, and therefore only the data corresponding to one of them are discussed. An ORTEP-type view of one of them is shown in Fig. 1, and selected bonding data are collected in the Table *S*1 (Supporting Information). The structure exhibits a distorted octahedral geometry around the ruthenium atom which is bonded to three nitrogen atoms of ^{i}Pr-pybox ligand, the nitrogen atom N^2 of pyrazole and two chlorine atoms. The chlorine atoms and the nitrogen atoms of pyridine and pyrazole groups are located in a *trans* disposition with both angle values close to the linearity (Cl(1)-Ru(1)-Cl(2) = 176.47(3)º; N(2)–Ru(1)–N(4) = 177.14(11)º). The Ru(1)–N(1) (2.107(3) Å), Ru(1)–N(2) (1.949(3) Å) and Ru(1)–N(3) (2.066(3) Å) distances as well as the N(1)–Ru(1)–N(2) (78.50(11)º), N(1)–Ru(1)–N(3) (156.88(11)º) and N(2)–Ru(1)–N(3) (78.37(11)º) bond angles fall in the range observed for other related ruthenium(II) pybox complexes [14,15]. The Ru(1)–N(4) distance (2.117(3) Å) is also in the range found for other ruthenium(II)-pyrazole complexes [16]. It is also observed from Fig. 1 the intramolecular hydrogen bond between the H(5 N) (distance N(5)-H(5 N), 0.92 Å) and one of the equatorial chlorine ligands. The distances N(5)···Cl(2) (3.1525(1) Å) and H(5 N)···Cl(2) (2.56 Å) as well as the angle value N(5)–H(5 N)···Cl(2) (122°) are consistent with the existence of a weak hydrogen bond [17]. On the other hand, the dihedral angle (α = 19.70(3)º), formed by the planes containing Ru(1)–N(4)–N(5)–H(5N) and Cl(2)–Ru(1)–Cl(1) moieties, appears to locate the N(5)–H(5N) vector in a such a way that the intramolecular hydrogen bond is facilitated [18].

*2.3. Synthesis of the complexes trans-[$OsCl_2$(L){(S,S)-^{i}Pr-pybox}] [L = py (**12**), 3-Br-py (**13**), 3-CN-py (**14**), 3-MeO-py (**15**), 3-NO_2-py (**16**), 4-CN-py (**17**), 4-MeO-py (**18**), isoquinoline (**19**), 1-methylimidazole (**20**), 1-benzylimidazole (**21**), pyrazole (**22**)]*

The synthesis of related osmium complexes containing six- and five-nitrogen heterocycles was also undertaken by ethylene-ligand exchange

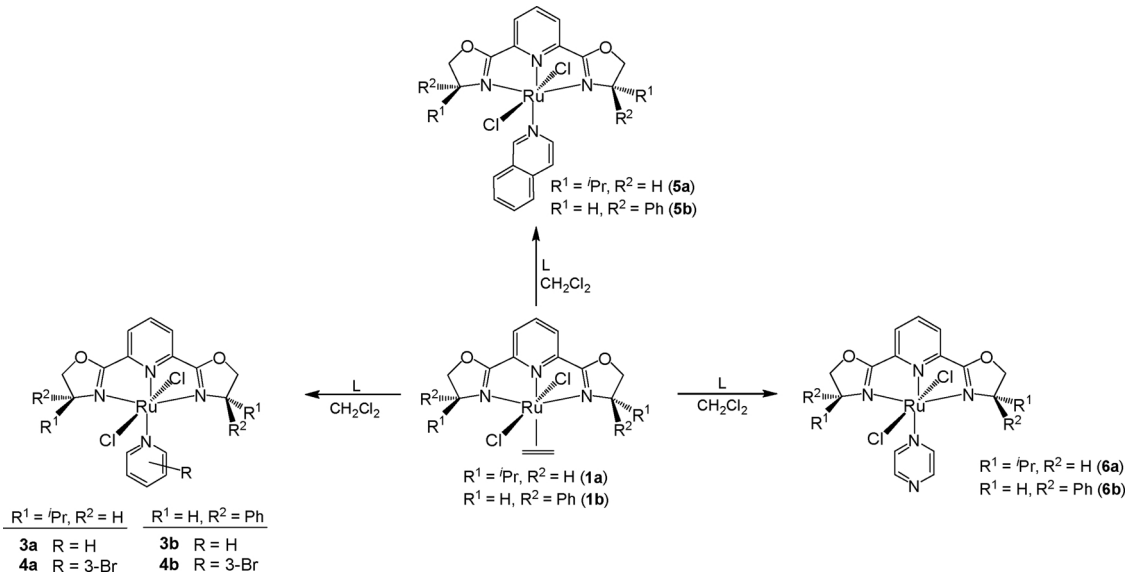

Scheme 1. Synthesis of complexes **3**-**6** by ligand exchange from complexes **1.**

(Schemes 3 and 4). Firstly, the osmium complex **2** was reacted with various pyridines and isoquinoline (1:1.5 M ratio) in refluxing toluene to give stereoselectively the *trans*-complexes **12–18** (74–93% yield) and **19** (91% yield), respectively (Scheme 3). The reaction works satisfactorily with pyridine itself as well as with electron-donor and -acceptor substituted pyridines. Unlike the case of ruthenium, the reaction of the complex **2** with pyrazine gives rise in all cases to a mixture of the mono- $[OsCl_2(C_4H_4N_2)(^i$Pr-pybox$)]$ and dinuclear $[(OsCl_2\{^i$Pr-pybox$\})_2(\mu$-*N*,*N*-$C_4H_4N_2)]$ complexes, even if large excess of pyrazine is used. However, under the appropriate conditions, the reaction can be exclusively directed to the dinuclear complex (see below).

In the same way, the reaction of the complex **2** with 1-methyl and 1-benzylimidazole as well as with pyrazole (1:1.5 M ratio, refluxing toluene) led to the complexes **20** (93% yield), **21** (89% yield) and **22** (74% yield), respectively (Scheme 4). The complexes **12–22** have been characterized by NMR spectroscopy; moreover, the ion molecular $[OsCl_2(L)(^i$Pr-pybox$)]^+$ is observed as the base peak in their mass spectra (ESI) (see Experimental Section).

The *trans* stereochemistry of complexes **12**-**22** can be readily evidenced by the ^{1}H and $^{13}C\{^1H\}$ NMR spectra (see the Experimental Section for further details). The structure of the complex **12** has been confirmed by a single crystal X-ray analysis. An ORTEP-type view of this complex and selected bonding data are shown in the Fig. 2 and the Table *S*2 (Supporting Information), respectively. The complex **12** exhibits a distorted octahedral geometry around the osmium atom which is bonded to the three nitrogen atoms of the pybox ligand, the nitrogen atom of pyridine and two chlorine atoms. The chlorine atoms Cl(1)-Os-Cl(2) (178.22(7)º) and the nitrogen atoms of both pyridine units N (2)–Os(1)–N(4) (178.5(3)º) are located in a *trans* arrangement with both angle values close to the linearity. The Os(1)–N(1) (2.068(6) Å), Os(1)–N(2) (1.946(6) Å) and Os(1)–N(3) (2.074(6) Å) distances, as well as the N(1)–Os(1)–N(2) (78.1(3)º), N(1)–Os(1)–N(3) (156.4(3)º) and N (2)–Os(1)–N(3) (78.4(3)º) bond angles, fall in the range observed for other related osmium(II) pybox complexes [19]. The osmium-pyridine nitrogen distance Os(1)–N(4) (2.134(6) Å) is also in the range found for other osmium(II)-pyridine complexes [20].

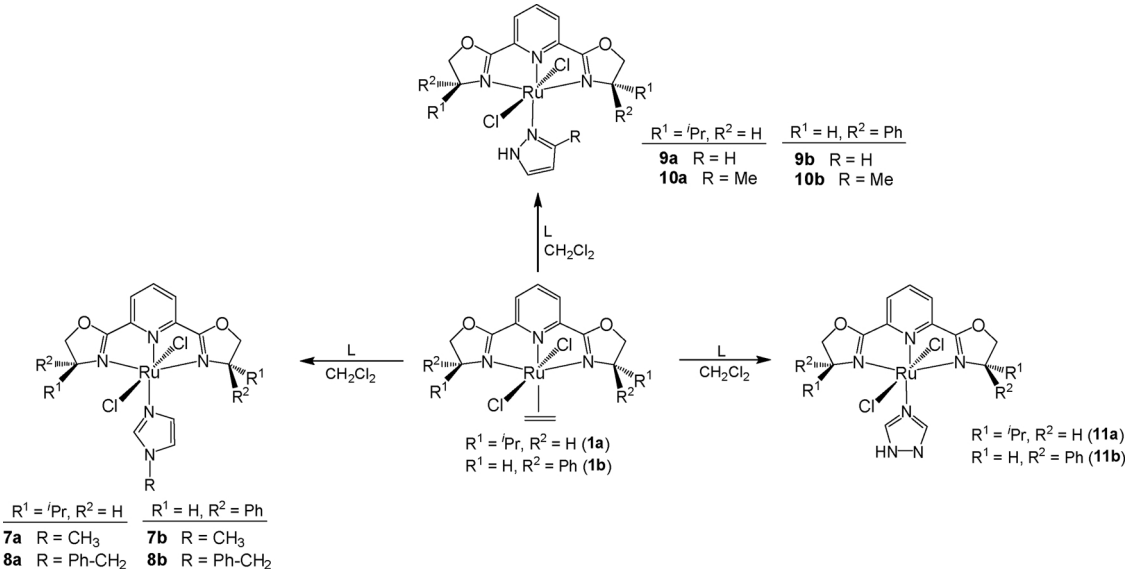

Scheme 2. Synthesis of complexes **7**-**11** by ligand exchange from complexes **1.**

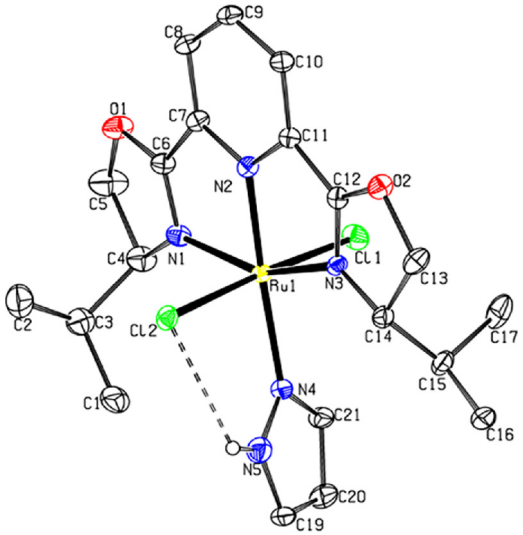

Fig. 1. ORTEP drawing of the complex **9a** showing atom-labeling scheme. Thermal ellipsoids are shown at the 30% probability level. With the exception of H(5N), the hydrogen atoms have been omitted for clarity.

2.4. Synthesis of the dinuclear complexes [{$RuCl_2$(R-pybox)}$_2$(μ-N,N-$C_4H_4N_2$)] (R = (S,S)-^{i}Pr (**23a**), (R,R)-Ph (**23b**)) and [($OsCl_2${(S,S)-^{i}Pr-pybox})$_2$(μ-N,N-$C_4H_4N_2$)] (**24**)

The use of dinitrogen heterocyclic ligands gave access to dinuclear ruthenium and osmium complexes (Scheme 5). Thus, the reaction of the ruthenium complexes **1a,b** with pyrazine (1:0.5 M ratio) in dichloromethane (reflux for **1a**; 60 °C, sealed tube for **1b**) provided the ruthenium complexes **23a,b** in 88–89 % yield. Moreover, the complexes **23a,b** are also readily accessible by the stoichiometric treatment of the single ruthenium-pyrazine complexes **6a,b** with the starting complexes **1a,b** with similar yields (see Experimental Section). Although the complex **23a** seems to exist as a mixture of two conformers in solution according to the ^{1}H and ^{13}C{^{1}H} NMR spectra, crystals could be obtained only for one conformer (see below). On the other hand, the reaction of the osmium complex **2** with pyrazine (1:1.5 M ratio) under refluxing toluene affords the dinuclear complex [($OsCl_2${(S,S)-^{i}Pr-pybox})$_2$(μ-N,N-$C_4H_4N_2$)] (**24**) (84% yield) (Scheme 5).

The structures of the complexes **23a** and **24** have been confirmed by a single crystal X-ray analysis. An ORTEP-type view of complexes **23a** and **24** and selected bonding data of both complexes are shown in Figs. 3 and 4 and in the Tables *S*3 and *S*4 (Supporting Information). The complexes **23a** and **24** show very similar dinuclear structures exhibiting two metal atoms bonded through a bridge pyrazine ligand. We observe the expected distorted octahedral coordination around each metal that is bonded to the three nitrogen atoms of pybox ligand, one of the nitrogen atoms of pyrazine and two chlorine atoms with a *trans* arrangement. The axial positions around each metal center are occupied by the pyrazine- and pyridine-nitrogen atoms. The Os-N distances and N-Os-N angles in the complex **24** are similar to those found in the osmium-pyridine complex **12**. The complex **23a** has an C_2-symmetry axis perpendicular to the pyrazine ring which generate half molecule from the other half. Therefore, the refinement of the structure has been carried out only for one half of the molecule (see Table *S*3). The complexes **23a**·Et_2O and **24**·$2CH_2Cl_2$ represent the first reported dinuclear ruthenium and osmium complexes containing pybox ligands.

2.5. Catalytic transfer hydrogenation of ketones

Recently we reported on the capability of pybox-ruthenium and -osmium complexes as catalysts for asymmetric transfer hydrogenation of ketones. Thus, we found that complexes of the type [MCl_2L(R-pybox)] (L = phosphorous ligand) are able to catalyze the reduction of different aryl ketones to secondary benzyl alcohols. Moreover, the efficiency of the asymmetric reduction depends not only on the metal and the chiral ligand but also on the nature of the achiral phosphorous ligand [12,13]. Thus, while the reaction works nicely (96–99% conversion, up to 95% *e.e.*) for *cis*-[$RuCl_2$(L){(*R,R*)-Ph-pybox}] (L = PR_3) and *trans*-[$OsCl_2$(L){(*S,S*)-^{i}Pr-pybox}] (L = $P(OR)_3$), significantly lower enantiomeric excess was reached for the corresponding $P(OR)_3$-ruthenium and PR_3-osmium complexes. Having in mind the different nature of *P-vs N*-ligands in coordination chemistry, we decided to explore the catalytic activity of the nitrogen complexes described above in the ATH of prochiral ketones.

Firstly, we tested the activity of selected ruthenium complexes in the asymmetric reduction of acetophenone under standard reaction conditions [21]. Unfortunately, the complexes *trans*-[$RuCl_2$(L)(R-pybox)] (R-pybox = (*S,S*)-^{i}Pr-pybox, L = pyridine (**3a**), pyrazine (**6a**), 3-methylpyrazole (**10a**); R-pybox = (*R,R*)-Ph-pybox, L = pyridine (**3b**), 3-methylpyrazole (**10b**)) were not able to catalyze the AHT reaction of acetophenone in an acceptable way (52–88% conversion; < 4% *e.e.*, Table 1). It was also observed that the conversion is significantly lower for Ru-pyrazole (53-52%, entries 4,5) than for Ru-pyridine and -pyrazine complexes (88–79%, entries 1–3). Further attempts to improve the chiral induction by modifying the general parameters, *e.g.* amount of catalyst and base, dilution and temperature, were also unsuccessful.

On the other hand, the osmium complexes appear to be more promising in the AHT reaction. Firstly, we selected the complex *trans*-[$OsCl_2$(py){(*S,S*)-^{i}Pr-pybox}] (**12**) since, i) the pyridine ligand was the best ligand in the case of ruthenium (see above), ii) it was earlier demonstrated that the isopropylpybox complexes are superior to the analogous phenylpybox complexes [13]. The Table 2 displays the results of the reduction of acetophenone, under different reaction conditions, using the osmium complex **12** as the catalyst and 2-propanol/base as the hydrogen source. Initially the following protocol was followed. The complex **12** (0.4 mol %) was added to a solution of

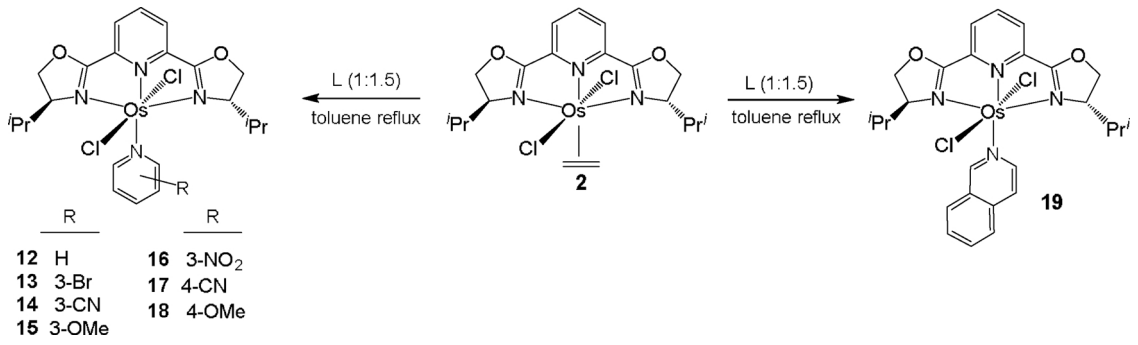

Scheme 3. Synthesis of complexes **12–19** by ligand exchange from **2.**

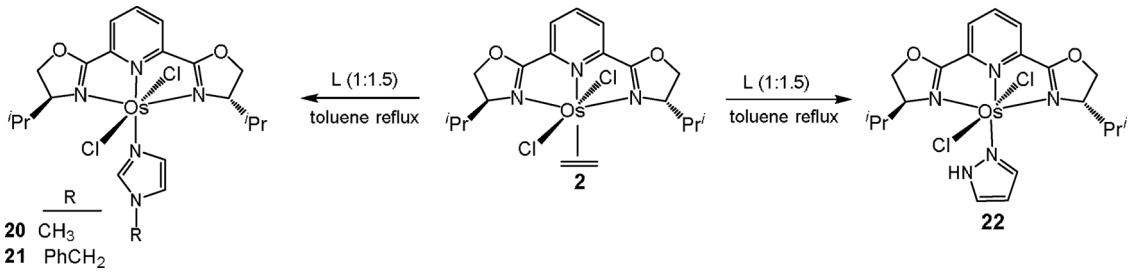

Scheme 4. Synthesis of complexes **20–22** by ligand exchange from **2.**

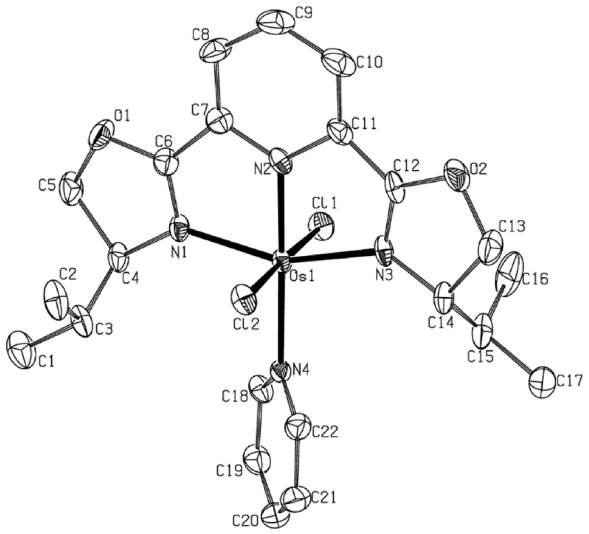

Fig. 2. ORTEP drawing of the complex **12** showing atom-labeling scheme. Thermal ellipsoids are shown at the 30% probability level. Hydrogen atoms are omitted for clarity.

acetophenone (2.5 mmol) in 2-propanol (70 mL) under an argon atmosphere and the mixture stirred for 15 min at 82 °C [22]. Then, 0.3 mmol of KO^{t}Bu (5 ml of a 0.06 M solution in 2-propanol) (ketone/catalyst/KO^{t}Bu ratio = 250:1:30) were added and the resulting mixture stirred for 4 h (monitored by gas chromatography) affording (*R*)-phenylethanol with 96% of conversion and 57% *e.e.* (Table 2, entry 1) [23]. It should be pointed that the efficiency of the analogous ruthenium complex **3a** is clearly inferior (88% of conversion and < 4% *e.e.*; see Table 1, entry 1).

It is well-known that transfer hydrogenation process is sensitive to the nature and concentration of the base [24,25]. Moreover, hydroxides, alkoxides and carbonates, at various concentrations, are commonly employed in these reactions [1j,26]. Therefore, the effect of the amount and nature of base was analyzed.

i) *Amount of base*: A dependence is observed on the catalyst/KO^{t}Bu molar ratio, the best result being obtained using a molar ratio of 1:30 (entry 1). Using a higher molar ratio (1:45) led to a similar conversion but lower *e.e.* (entry 2 *vs* 1). On the other hand, a lower molar ratio (1:15) gave rise to lower conversion and *e.e.* (entry 3 *vs* 1). ii) *Nature of base*: Based on the protocol of entry 1, a number of different bases were explored (entries 4–8). We found that both conversion and asymmetric induction using the bases NaO^{t}Bu, KOH, NaOH and KHDMS (entries 4–7) were clearly inferior to those reached with KO^{t}Bu. On the

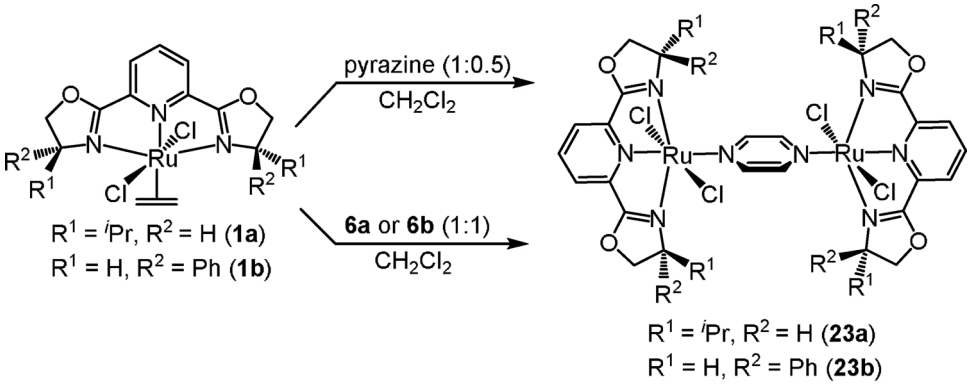

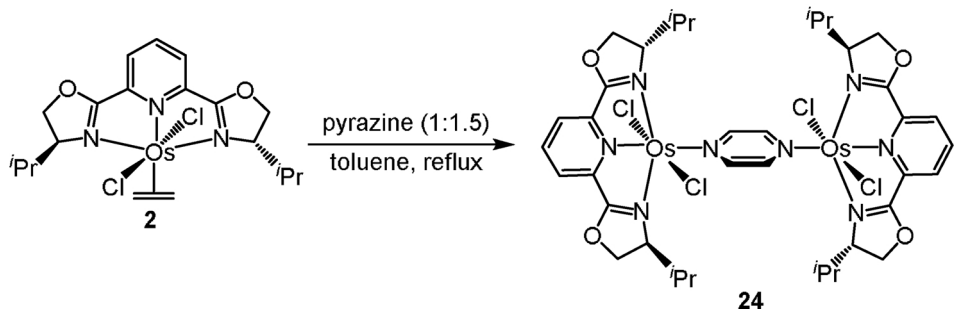

Scheme 5. Synthesis of dinuclear complexes **23a**,**b** and **24.**

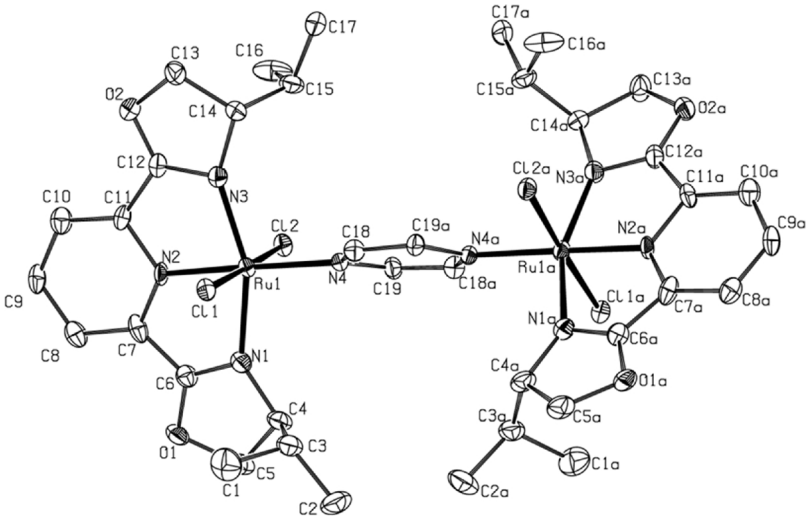

Fig. 3. ORTEP drawing of the dinuclear complex **23a** showing atom-labeling scheme. Thermal ellipsoids are shown at the 30% probability level. Hydrogen atoms are omitted for clarity.

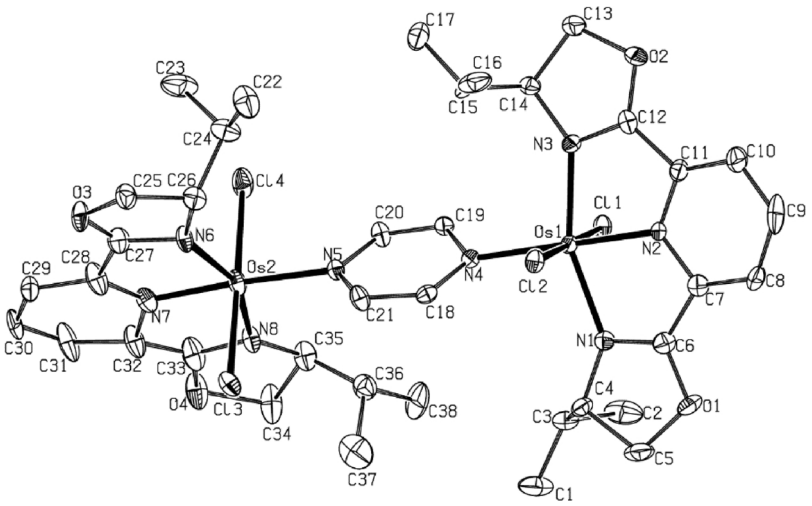

Fig. 4. ORTEP drawing of the dinuclear complex **24** showing atom-labeling scheme. Thermal ellipsoids are shown at the 10% probability level. Hydrogen atoms are omitted for clarity.

Table 1
Transfer Hydrogenation of Acetophenone Catalyzed by Ruthenium Complexes *trans*-[RuCl2(L){(S,S)-^{i}Pr-pybox}] (**3a**, **6a**, **10a**) and *trans*-[$RuCl_2$(L){(*R*,*R*)-Ph-pybox}] (**3b**, **10b**).[a]

	Catalyst	time, *t* (h)	Conversion (%)[b]
1	**3a** (L = pyridine)	4	88
2	**3b** (L = pyridine)	4	79
3	**6a** (L = pyrazine)	4	86
4	**10a** (L = 3-methylpyrazole)	4	53
5	**10b** (L = 3-methylpyrazole)	4	52

[a]Reactions were carried out at 82 °C using 5 mmol of acetophenone, 0.2 mol % catalyst, KO^{t}Bu and 2-propanol (50 mL) (ketone/catalyst/ KO^{t}Bu ratio: 500:1:24); [b]Determined by GC with a Supelco *β*-DEX 120 chiral capillary column.

contrary, Cs_2CO_3 proved to be superior in terms of asymmetric induction, while the conversion dropped from 96 to 78% (entry 8 *vs* entry 1). On the other hand, the conversion could be improved without loss of asymmetric induction by extending the reaction time from 4 to 7 h. Thus, analogous conversion (94 *vs* 96%) and higher *e.e.* (64 *vs* 57%) were reached with cesium carbonate (entry 9) than with potassium *tert*butoxide (entry 1).

Finally, entry 10 displays a further optimization by varying the concentration of reactants and reaction time given in entry 9. Thus, using 50 ml of 2-propanol ([ketone] = 0.05 mmol/mL) instead of 75 ml of 2-propanol ([ketone] = 0.034 mmol/mL) allows to revers the reaction time from 7 to 4 h although similar conversion (93 *vs* 94%) and *e.e.* (64 *vs* 64%) was observed. These optimized reaction conditions (ketone/catalyst/ Cs_2CO_3 ratio: 250:1:30, 50 ml of 2-propanol) are employed for the rest of the osmium catalytic reactions reported below (variations of nitrogen ligand: Tables *S*5, *S*6; reduction of ketones: Table 3).

In addition, we have checked the reduction of acetophenone with complexes bearing some other six-membered nitrogen ligands. We found that the complexes with 3-methoxy- **15**, 3-nitro- **16**, 4-methoxypyridine **18**, as well the pyrazine dinuclear complex **24**, behaved somewhat less efficient that the pyridine complex **12** under the optimized reaction conditions (acetophenone/catalyst/$CsCO_3$ ratio: 250:1:30, 50 ml 2-propanol) (reaction time 4 h, 42–82% conversion, 50–61% *e.e.*; see Table *S*5, Supporting Information). The other complexes **13**, **14**, **17**, and **19** (L = 3-bromo-, 3-cyano, 4-cyanopyridine, and isoquinoline, respectively) provided < 43% *e.e.* (see Table *S*5,

Table 2
Transfer Hydrogenation of Acetophenone Catalyzed by Osmium Complex *trans*-[$OsCl_2$(py){(*S*,*S*)-^{i}Pr-pybox}] (**12**)[a].

	ketone/ catalyst/ base ratio	Base	time, *t* (h)	Conversion (%)[b]	*e.e.* (%)[b] (*R*)	TOF (h^{-1})[c]
1	250:1:30	KO^{t}Bu	4	96	57	115
2	250:1:45	KO^{t}Bu	4	95	47	110
3	250:1:15	KO^{t}Bu	4	73	48	80
4	250:1:30	NaO^{t}Bu	4	81	46	90
5	250:1:30	KOH	4	70	55	55
6	250:1:30	NaOH	4	80	46	90
7	250:1:30	KHDMS	4	68	53	60
8	250:1:30	Cs_2CO_3	4	78	62	50
9	250:1:30	Cs_2CO_3	7	94	64	50
10[d]	250:1:30	Cs_2CO_3	4	93	64	110

[a] Reactions were carried out at 82 °C using 2.5 mmol of acetophenone, 0.4 mol % catalyst and 2-propanol (75 mL).
[b] Determined by GC with a Supelco *β*-DEX 120 chiral capillary column.
[c] TOF at $t = 30$ min.
[d] Reaction was carried out at 82 °C using 2.5 mmol of acetophenone, 0.4 mol % catalyst and 2-propanol (50 mL).

Table 3
Selected Examples of Transfer Hydrogenation of Aryl Ketones Catalyzed by Osmium Complexes[a].

	Ketone	catalyst	*t* (h)	conv. (%)	e.e. (%) (*R*)[b]	TOF (h^{-1})[c]
1		**12**	4	93	64	110
2		**12**	3	97	68	95
3		**12**	6	94	73	75
4		**16**	5	11	33	40[d]
5		**12**	4	97	63	80
6		**12**	10	95	55	50
7		**12**	10	91	46[e]	50
8[f]		**24**	4	96	59	105
9[f]		**24**	7	93	64	85
10	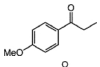	**15**	6	93	66	70
11		**15**	5	95	60	50

[a] Reactions were carried out at 82 °C using 2.5 mmol of ketone, 0.4 mol% catalyst, Cs_2CO_3 and 2-propanol (50 mL) (ketone/catalyst/Cs2CO3 ratio: 250:1:30).
[b] Determined by GC with a Supelco *β*-DEX 120 chiral capillary column.
[c] TOF at $t = 30$ min.
[d] TOF at $t = 2.5$ h.
[e] The S-enantiomer is the major isomer.
[f] Reaction was carried out using 0.2 mol% of the dimer catalyst (ketone/catalyst/Cs_2CO_3 ratio: 250:0.5:30).

Supporting Information). From these data, it seems clear that the presence of substituents at the pyridine ring, with either donating- (**18**) or withdrawing-electron (**13**-**17**) properties, lowers the efficiency of the reduction with respect to the pyridine itself **12**. These results, along with those found in the cases of isoquinoline **19** and dinuclear pyrazine **24**, suggest that the major influence of the nitrogen-heterocyclic ligand is due to steric effects rather than to electronic factors (see Table S5, Supporting Information).

On the other hand, we have checked the complexes bearing a five-membered nitrogen ligand as 1-methylimidazole **20**, 1-benzylimidazole **21**, and pyrazole **22.** In all cases, they provided low-to-moderate conversions (60–83%) and poor enantiomeric excess (< 34%) (see Table *S*6, Supporting Information).

Finally, based on the optimized conditions defined in the reduction of acetophenone with the pyridine osmium catalyst, the AHT reduction of different aryl ketones was performed using the precatalyst complexes **12**, **15**, **16**, **18** and **24.** The best catalyst, as well as the optimized reaction time, for the reduction of each ketone is shown in Table 3 (for more detailed results, see Table *S*7 in the Supporting Information). With the exception of 2-bromoacetophenone (entry 4), all of the reductions take place with conversions up to 90%. The highest *e.e.* values (63–73%) are obtained in the reduction of acetophenone (64%, entry 1), propiophenone (68%, entry 2), isobutyrophenone (73%, entry 3), 3-bromoacetophenone (63%, entry 5), 4-methoxyacetophenone (64%, entry 9) and 4-methoxypropiophenone (66%, entry 10).

These results are interesting in terms of comparison of osmium catalysis *versus* ruthenium catalysis. Specifically, herein it is shown for the first time that the catalytic activity of osmium complexes in the asymmetric transfer hydrogenation (ATH) of ketones is superior to that of the ruthenium counterparts. To the best of our knowledge, a sole precedent dealing with a non-asymmetric ketone reduction catalyzed by an achiral osmium(II) complex was reported by S. Chattopadhyay and col. They found that the reduction of a number of ketones with the achiral osmium(II) complex [OsBr(NNO)(CO)(PPh_3)] (NNO = 1-{[2phenylazo)phenyl]iminomethyl}-2-phenolate) takes place with moderate-to-high yield while the related ruthenium complex shows no activity [27].

3. Conclusion

A series of enantiopure pybox-ruthenium (**3a**,**b-11a**,**b)** and -osmium (**12–22**) complexes bearing a N-heterocyclic ligand has been prepared from **1**,**2** by ethylene ligand exchange with pyridine derivatives, 1,4-diazine, pyrazole, imidazole and triazole. The dinuclear complexes of Ru (**23a**,**b)** and Os (**24)** have also been prepared from 1,4-diazine. Most of the complexes prepared have been tested as catalysts in the AHT reaction. The ruthenium complexes show lower efficiency than the osmium analogs in the AHT reduction of acetophenone, particularly in terms of asymmetric induction (< 4% *e.e. vs* < 64% *e.e.* The reduction of a variety of alkylarylketones has been undertaken with the osmium complexes *trans*-[$OsCl_2$(L){(*S*,*S*)-^{i}Pr-pybox}] (L = py (**12**), 3-MeO-py (**15**), 3-NO_2-py (**16**), 4-MeO-py (**18**)) and [($OsCl_2${(*S*,*S*)-^{i}Pr-pybox})$_2$(μ-*N*,*N*-$C_6H_4N_2$)] (**24**) with high conversion (up to 90%) and moderate enantioselectivity (63–73% *e.e.*).

These results confirm, in our opinion, the potential of both osmium and ruthenium complexes for the design of new highly productive and robust catalysts for the synthesis of chiral alcohols. Although the capability of Ru-pybox and Os-pybox complexes for the AHT reduction is well recognized [12,13], we show herein that the efficiency of osmium complexes is superior to that of ruthenium complexes in the AHT reduction of ketones using M/pybox/pyridine catalysts. This reflects that the catalytic activity of Os and Ru complexes can be complementary.

4. Experimental

4.1. General procedures

The reactions were performed under an atmosphere of dry argon using vacuum-line and standard Schlenk techniques. Pyridine, acetophenone and propiophenone were destilled before use. The rest of reagents were obtained from commercial suppliers and used without further purification. Solvents were dried by standard methods and

distilled under argon before use. The precursors *trans*-[$OsCl_2(\eta^2$-C_2H_4){(*S*,*S*)-^{i}Pr-pybox}] [14], *trans*-[$RuCl_2(\eta^2$-C_2H_4){(*S*,*S*)-^{i}Pr-pybox}] and *trans*-[$RuCl_2(\eta^2$-C_2H_4){(*R*,*R*)-Ph-pybox}] [28] were synthesized by reported methods. Infrared spectra were recorded on a Perkin-Elmer 1720-XFT spectrometer. The C, H, N analyses for ruthenium/Ph-Pybox complexes (**3b-11b**, **23b**) were carried out with a LECO CHNS-TruSpec microanalyzer. Inconsistent analyses were found for ruthenium-^{i}Pr-pybox and osmium complexes due to incomplete combustion. For these complexes, **4a–11a**, **23a** (^{i}Pr-pybox/ruthenium) and **12–22**, **24** (^{i}Pr-pybox/osmium), mass spectra (ESI) were determined with a Bruker Esquire 6000 spectrometer, operating in positive mode and using dichloromethane/methanol solutions and an Agilent 6460 spectrometer (LC−MS of triple quadrupole), operating in positive mode and using acetonitrile/water (50:50) solutions with 0.1% of formic acid. NMR spectra were recorded on Bruker spectrometers (AV-300 operating at 300.13 (^{1}H) MHz; AV 400 operating at 400.13 (^{1}H) and 100.62 (^{13}C) MHz). DEPT and/or bidimensional HSQC experiments were carried out for all the complexes. The ^{1}H and ^{13}C{^{1}H}NMR spectra for all the complexes reported are provided as Supporting Information. Chemical shifts are reported in parts per million and referenced to TMS as standard. Coupling constants *J* are given in hertz. Abbreviations used: s, singlet; br s, broad singlet; d, doublet; dd double doublet; t, triplet; pt, pseudo triplet; m, multiplet. The following atom labels have been used for the ^{1}H and ^{13}C{^{1}H} spectroscopic data of the pybox ligand.

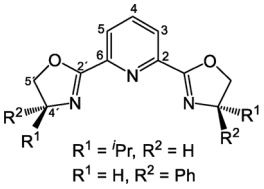

4.2. Synthesis of the complexes trans-[$RuCl_2$(L){(*S*,*S*)-^{i}Pr-pybox}] (L = pyridine (**3a**), 3-bromopyridine (**4a**), isoquinoline (**5a**), pyrazine (**6a**), 1-methylimidazole (**7a**), 1-benzylimidazole (**8a**), pyrazole (**9a**), 3-methylpyrazole (**10a**), 1H-1,2,4-triazole (**11a**)

A solution of complex *trans*-[$RuCl_2(\eta^2$-C_2H_4){(*S*,*S*)-^{i}Pr-pybox)] (**1a**) (0.030 g, 0.06 mmol) and the *N*-donor ligand (0.09 mmol) in dichloromethane (10 mL) was heated under reflux conditions for 4.5 h. The solvent was then removed under vacuum. The addition of diethyl ether produced the precipitation of the corresponding complex. The solvent was decanted and the solid was washed with diethyl ether (3 x 5 mL) and vacuum-dried.

Complex **3a**: Yield 88% (29 mg, 0.053 mmol). Color: dark purple. ^{1}H NMR (300.13 MHz, $CDCl_3$, 298 K): δ = 9.84 (d, J_{HH} = 5.4 Hz, 2H, C_6H_5N), 7.89 (t, J_{HH} = 7.8 Hz, 1H, H^4 C_5H_3N), 7.69 (d, J_{HH} = 7.8 Hz, 2H, H^{3,5} C_5H_3N), 7.52 (m, 3H, C_6H_5N), 4.89 (pt, J_{HH} = 8.7 Hz, 2H, OCH_2), 4.77 (pt, J_{HH} = 8.7 Hz, 2H, OCH_2), 4.23 (m, 2H, C*H*^{i}Pr), 1.71 (m, 2H, C*H*Me_2), 0.78 (d, J_{HH} = 6.7 Hz, 6H, CH*Me*$_2$), 0.73 (d, *J* = 6.7 Hz, 6H, CH*Me*$_2$) ppm. ^{1}H NMR data are in accordance with the values previously reported for this complex [29].

Complex **4a**: Yield 87% (33 mg, 0.052 mmol). Color: dark purple. Exact mass for $C_{22}H_{27}BrCl_2N_4O_2Ru$ (629.97). MS-ESI: *m/z* = 631.36 ([$RuCl_2(C_5H_4NBr)$(^{i}Pr-pybox) + 1]$^+$, 100%). ^{1}H NMR (300.13 MHz, $CDCl_3$, 298 K): δ = 9.96 (m, 1H, Br-C_5H_4N), 9.77 (m, 1H, Br-C_5H_4N), 8.02 (m, 1H, Br-C_5H_4N), 7.71 (m, 2H, H^{3,5} C_5H_3N), 7.58 (m, 1H, H^4 C_5H_3N), 7.28 (m, 1H, Br-C_5H_4N), 4.89 (m, 2H, OCH_2), 4.79 (m, 2H, OCH_2), 4.25 (m, 2H, C*H*^{i}Pr), 1.70 (m, 2H, C*H*Me_2), 0.83 (d, J_{HH} = 6.3 Hz, 6H, CH*Me*$_2$), 0.74 (d, J_{HH} = 6.3 Hz, 6H, CH*Me*$_2$) ppm. ^{13}C{^{1}H} NMR (100.62 MHz, $CDCl_3$, 298 K): δ = 166.1 (s, OCN), 157.0, 154.3 (2*s*, CH Br-C_5H_4N), 151.6 (s, C^{2,6} C_5H_3N), 138.5 (s, CH Br-C_5H_4N), 128.4 (s, C^4 C_5H_3N), 124.5 (s, CH Br-C_5H_4N), 123.0 (s, C^{3,5} C_5H_3N), 119.9 (s, C Br-C_5H_4N), 71.5 (s, OCH_2), 68.9 (s, C*H*^{i}Pr), 29.9 (s, *C*HMe_2), 19.3, 15.5 (2*s*, CH*Me*$_2$) ppm.

Complex **5a**: Yield 98% (35 mg, 0.059 mmol). Color: dark purple. Exact mass for $C_{26}H_{30}Cl_2N_4O_2Ru$ (602.08). MS-ESI: *m/z* = 602.08 ([$RuCl_2(C_9H_7N)$(^{i}Pr-pybox)]$^+$, 100%). ^{1}H NMR (300.13 MHz, CD_2Cl_2, 298 K): δ = 10.48 (s, 1H, C_9H_7N), 9.69 (d, J_{HH} = 6.3 Hz, 1H, C_9H_7N), 8.16 (d, J_{HH} = 7.8 Hz, 1H, C_9H_7N), 8.04 (m, 1H, C_9H_7N), 7.91-7.57 (m, 6H, H^{3,4,5} C_5H_3N, C_9H_7N), 4.92 (m, 2H, OCH_2), 4.81 (m, 2H, OCH_2), 4.33 (m, 2H, C*H*^{i}Pr), 1.66 (m, 2H, C*H*Me_2), 0.72 (d, J_{HH} = 6.9 Hz, 6H, CH*Me*$_2$), 0.65 (d, J_{HH} = 6.6 Hz, 6H, CH*Me*$_2$) ppm. ^{13}C{^{1}H} NMR (100.62 MHz, $CDCl_3$, 298 K): δ = 166.1 (s, OCN), 159.0 (s, CH C_9H_7N), 151.8 (s, C^{2,6} C_5H_3N), 148.1 (s, CH C_9H_7N), 135.2-126.5 (CH C_9H_7N, C C_9H_7N, C^4 C_5H_3N), 122.8 (s, C^{3,5} C_5H_3N), 120.4 (s, CH C_9H_7N), 71.4 (s, OCH_2), 69.1 (s, C*H*^{i}Pr), 29.7 (s, *C*HMe_2), 19.3, 15.4 (2*s*, CH*Me*$_2$) ppm.

Complex **6a**: Yield 92% (31 mg, 0.055 mmol). Color: dark purple. Exact mass for $C_{21}H_{27}Cl_2N_5O_2Ru$ (553.06). MS-ESI: *m/z* = 553.1 ([$RuCl_2(C_4H_4N_2)$(^{i}Pr-pybox)]$^+$, 100%). ^{1}H NMR (400.13 MHz, $CDCl_3$, 298 K): δ = 9.96 (s, 2H, $C_4H_4N_2$), 8.66 (s, 2H, $C_4H_4N_2$), 7.73 (d, J_{HH} = 8.0 Hz, 2H, H^{3,5} C_5H_3N), 7.63 (t, J_{HH} = 8.0 Hz, 1H, H^4 C_5H_3N), 4.88 (m, 2H, OCH_2), 4.76 (m, 2H, OCH_2), 4.20 (m, 2H, C*H*^{i}Pr), 1.60 (m, 2H, C*H*Me_2), 0.78 (d, J_{HH} = 7.2 Hz, 6H, CH*Me*$_2$), 0.73 (d, J_{HH} = 6.8 Hz, 6H, CH*Me*$_2$) ppm. ^{13}C{^{1}H} NMR (100.62 MHz, $CDCl_3$, 298 K): δ = 165.8 (s, OCN), 151.0 (s, $C_4H_4N_2$, C^{2,6} C_5H_3N), 150.1 (s, C^{2,6} C_5H_3N), 144.7 (s, $C_4H_4N_2$), 129.7 (s, C^4 C_5H_3N), 122.9 (s, C^{3,5} C_5H_3N), 71.6 (s, OCH_2), 69.1 (s, *C*H^{i}Pr), 30.0 (s, *C*HMe_2), 19.1, 15.4 (2 s, CH*Me*$_2$) ppm.

Complex **7a**: Yield 66% (22 mg, 0.040 mmol). Color: dark purple. Exact mass for $C_{21}H_{29}Cl_2N_5O_2Ru$ (555.07). MS-ESI: *m/z* = 555.1 ([$RuCl_2(C_4H_6N_2)$(^{i}Pr-pybox)]$^+$, 100%). ^{1}H NMR (400.13 MHz, $CDCl_3$, 298 K): δ = 8.57 (s, 1H, NCHCHN), 8.14 (s, 1H, NCHCHN), 7.49-7.42 (m, 3H, H^{3,4,5} C_5H_3N), 7.11 (s, 1H, NCHN), 4.90 (pt, J_{HH} = 8.5 Hz, 2H, OCH_2), 4.71 (pt, J_{HH} = 8.5 Hz, 2H, OCH_2), 4.14 (m, 2H, C*H*^{i}Pr), 3.91 (s, 3H, NCH_3), 1.79 (m, 2H, C*H*Me_2), 0.79 (d, J_{HH} = 6.8 Hz, 6H, CH*Me*$_2$), 0.76 (d, J_{HH} = 6.8 Hz, 6H, CH*Me*$_2$) ppm. ^{13}C{^{1}H} NMR (100.62 MHz, $CDCl_3$, 298 K): δ = 167.1 (s, OCN), 151.4 (s, C^{2,6} C_5H_3N), 140.5, 132.6 (2 s, NCHCHN), 125.3 (s, C^4 C_5H_3N), 123.2 (s, C^{3,5} C_5H_3N), 120.2 (s, NCHN), 71.1 (s, OCH_2), 69.3 (s, *C*H^{i}Pr), 34.3 (s, NCH_3), 29.4 (s, *C*HMe_2), 19.3, 15.5 (2 s, CH*Me*$_2$) ppm.

Complex **8a**: Yield 93% (35 mg, 0.056 mmol). Color: dark pink. Exact mass for $C_{27}H_{33}Cl_2N_5O_2Ru$ (631.11). MS-ESI: *m/z* = 631.2 ([$RuCl_2(C_{10}H_{10}N_2)$(^{i}Pr-pybox)]$^+$, 100%). ^{1}H NMR (400.13 MHz, $CDCl_3$, 298 K): δ = 8.74 (s, 1H, NCHCHN), 8.20 (s, 1H, NCHCHN), 7.53-7.28 (m, 8H, H^{3,4,5} C_5H_3N, Ph), 7.18 (s, 1H, NCHN), 5.15 (s, 2H, NCH_2), 4.88 (pt, J_{HH} = 8.5 Hz, 2H, OCH_2), 4.71 (pt, J_{HH} = 8.5 Hz, 2H, OCH_2), 4.18 (m, 2H, C*H*^{i}Pr), 1.78 (m, 2H, C*H*Me_2), 0.76 (m, 12H, CH*Me*$_2$) ppm. ^{13}C{^{1}H} NMR (100.62 MHz, $CDCl_3$, 298 K): δ = 168.4 (s, OCN), 151.1 (s, C^{2,6} C_5H_3N), 140.1 (s, NCHCHN), 136.4 (s, C^{ipso} Ph), 132.7 (s, NCHCHN), 129.2-127.2 (Ph), 125.1 (s, C^4 C_5H_3N), 123.7 (s, C^{3,5} C_5H_3N), 119.6 (s, NCHN), 71.1 (s, OCH_2), 69.2 (s, *C*H^{i}Pr), 51.9 (s, NCH_2), 29.6 (s, *C*HMe_2), 19.4, 16.0 (2 s, CH*Me*$_2$) ppm.

Complex **9a**: Yield 97% (32 mg, 0.059 mmol). Color: dark pink. Exact mass for $C_{20}H_{27}Cl_2N_5O_2Ru$ (541.06). MS-ESI: *m/z* = 541.1 ([$RuCl_2(C_3H_4N_2)$(^{i}Pr-pybox)]$^+$, 100%). ^{1}H NMR (400.13 MHz, $CDCl_3$, 298 K): δ = 12.56 (s, 1H, NH), 8.77 (s, 1H, CH $C_3H_4N_2$), 7.96 (s, 1H, CH $C_3H_4N_2$), 7.65 (d, J_{HH} = 7.6 Hz, 2H, H^{3,5} C_5H_3N), 7.50 (t, J_{HH} = 7.6 Hz, 1H, H^4 C_5H_3N), 6.68 (s, 1H, CH $C_3H_4N_2$), 4.80 (pt, J_{HH} = 8.6 Hz, 2H, OCH_2), 4.67 (pt, J_{HH} = 8.6 Hz, 2H, OCH_2), 4.01 (m, 2H, C*H*^{i}Pr), 1.65 (m, 2H, C*H*Me_2), 0.77 (d, J_{HH} = 6.8 Hz, 6H, CH*Me*$_2$), 0.76 (d, J_{HH} = 7.2 Hz, 6H, CH*Me*$_2$) ppm. ^{13}C{^{1}H} NMR (100.62 MHz, $CDCl_3$, 298 K): δ = 166.5 (s, OCN), 152.5 (s, C^{2,6} C_5H_3N), 142.5, 129.0 (2 s, $C_3H_4N_2$), 127.3 (s, C^4 C_5H_3N), 122.9 (s, C^{3,5} C_5H_3N), 107.0 (s, $C_3H_4N_2$), 71.5 (s, OCH_2), 69.8 (s, *C*H^{i}Pr), 29.2 (s, *C*HMe_2), 19.3, 15.6 (2 s, CH*Me*$_2$) ppm.

Complex **10a**: Yield 96% (32 mg, 0.058 mmol). Color: dark pink. Exact mass for $C_{21}H_{29}Cl_2N_5O_2Ru$ (555.07). MS-ESI: *m/z* = 555.1 ([$RuCl_2(C_4H_6N_2)$(^{i}Pr-pybox)]$^+$, 100%). ^{1}H NMR (400.13 MHz, $CDCl_3$,

298 K): δ = 12.07 (s, 1H, NH), 8.59 (s, 1H, CH $C_4H_6N_2$), 7.65 (d, J_{HH} = 8.8 Hz, 2H, $H^{3,5}$ C_5H_3N), 7.49 (t, J_{HH} = 8.8 Hz, 1H, H^4 C_5H_3N), 6.38 (s, 1H, CH $C_4H_6N_2$), 4.80 (pt, J_{HH} = 8.8 Hz, 2H, OCH_2), 4.67 (pt, J_{HH} = 8.8 Hz, 2H, OCH_2), 4.04 (m, 2H, C*H*^{i}Pr), 2.36 (s, 3H, CH_3), 1.71 (m, 2H, C*H*Me$_2$), 0.79 (d, J_{HH} = 7.2 Hz, 6H, CH*Me*$_2$), 0.78 (d, J_{HH} = 6.8 Hz, 6H, CH*Me*$_2$) ppm. $^{13}C\{^1H\}$ NMR (100.62 MHz, $CDCl_3$, 298 K): δ = 166.5 (s, OCN), 152.6 (s, $C^{2,6}$ C_5H_3N), 143.3 (s, CH $C_4H_6N_2$), 139.8 (s, *C*CH$_3$), 127.1 (s, C^4 C_5H_3N), 122.9 (s, $C^{3,5}$ C_5H_3N), 106.3 (s, CH $C_4H_6N_2$), 71.4 (s, OCH_2), 69.7 (s, *C*H^{i}Pr), 29.1 (s, *C*HMe$_2$), 19.4, 15.6 (2 s, CH*Me*$_2$), 11.2 (s, CH_3) ppm.

Complex **11a**: Yield 95% (31 mg, 0.057 mmol). Color: dark pink. Exact mass for $C_{19}H_{26}Cl_2N_6O_2Ru$ (542.05). MS-ESI: *m/z* = 542.1 ($[RuCl_2(C_2H_3N_3)(^i$Pr-pybox)$]^+$, 100%). ^1H NMR (400.13 MHz, $CDCl_3$, 298 K): δ = 13.53 (s, 1H, NH), 9.24 (s, 1H, $C_2H_3N_3$), 8.65 (s, 1H, $C_2H_3N_3$), 7.69 (m, 2H, $H^{3,5}$ C_5H_3N), 7.49 (m, 1H, H^4 C_5H_3N), 4.83 (m, 2H, OCH_2), 4.69 (m, 2H, OCH_2), 4.05 (m, 2H, C*H*^{i}Pr), 1.60 (m, 2H, C*H*Me$_2$), 0.82 (m, 12H, CH*Me*$_2$) ppm. $^{13}C\{^1H\}$ NMR (100.62 MHz, $CDCl_3$, 298 K): δ = 166.6 (s, OCN), 154.4 (s, $C_2H_3N_3$), 152.0 (s, $C^{2,6}$ C_5H_3N), 143.5 (s, $C_2H_3N_3$), 128.2 (s, C^4 C_5H_3N), 123.2 (s, $C^{3,5}$ C_5H_3N), 71.6 (s, OCH_2), 69.9 (s, *C*H^{i}Pr), 29.5 (s, *C*HMe$_2$), 19.5, 15.6 (2 s, CH*Me*$_2$) ppm.

*4.3. Synthesis of the complexes trans-[RuCl$_2$(L){(R,R)-Ph-pybox}] (L = pyridine (**3b**), 3-bromopyridine (**4b**), isoquinoline (**5b**), pyrazine (**6b**), 1-methylimidazole (**7b**), 1-benzylimidazole (**8b**), pyrazole (**9b**), 3-methylpyrazole (**10b**), 1H-1,2,4-triazole (**11b**))*

A solution of complex *trans*-[$RuCl_2(\eta^2$-C_2H_4){(*R*,*R*)-Ph-pybox)] (**1b**) (0.030 g, 0.05 mmol) and the *N*-donor ligand (0.10 mmol) in dichloromethane (10 mL) was heated at 55 °C in a sealed tube for 5.5 h. The solution was transferred to a Schlenk and the solvent was then removed under vacuum. The addition of diethyl ether (25 mL) produced the precipitation of the corresponding complex. The solvent was decanted and the solid was washed with diethyl ether (3 x 5 mL) and vacuum-dried.

Complex **3b**: Yield 81% (25 mg, 0.040 mmol). Color: dark purple. Anal. Calc. for $C_{28}H_{24}Cl_2N_4O_2Ru$ (620.50): C, 54.20; H, 3.90; N, 9.03. Found: C, 54.22; H, 4.05; N, 8.79. ^1H NMR (400.13 MHz, $CDCl_3$, 298 K): δ = 8.69 (d, J_{HH} = 6.8 Hz, 2H, C_5H_5N), 7.79 (d, J_{HH} = 8.4 Hz, 2H, $H^{3,5}$ C_5H_3N), 7.60 (t, J_{HH} = 8.4 Hz, 1H, H^4 C_5H_3N), 7.25 (t, J_{HH} = 8.4 Hz, 1H, C_5H_5N), 7.18-7.15 (m, 10H, Ph), 6.58 (dd, J_{HH} = 8.4 Hz, J_{HH} = 6.8 Hz, 2H, C_5H_5N), 5.24 (pt, J_{HH} = 8.4 Hz, 2H, OCH_2), 5.14 (pt, J_{HH} = 8.4 Hz, 2H, C*H*Ph), 4.56 (pt, J_{HH} = 8.4 Hz, 2H, OCH_2) ppm. $^{13}C\{^1H\}$ NMR (100.62 MHz, $CDCl_3$, 298 K): δ = 168.1 (s, OCN), 155.1 (s, CH C_5H_5N), 152.1 (s, $C^{2,6}$ C_5H_3N), 137.6 (s, C^{ipso} Ph), 134.1 (s, C_5H_5N), 128.3-128.1 (Ph), 127.6 (s, C^4 C_5H_3N), 123.4 (s, $C^{3,5}$ C_5H_3N), 122.2 (s, C_5H_5N), 78.4 (s, OCH_2), 69.1 (s, *C*HPh) ppm.

Complex **4b**: Yield 62% (22 mg, 0.031 mmol). Color: dark purple. Anal. Calc. for $C_{28}H_{23}Cl_2N_4O_2BrRu$ (699.39): C, 48.09; H, 3.31; N, 8.01. Found: C, 48.49; H, 3.40; N, 7.93. ^1H NMR (400.13 MHz, $CDCl_3$, 298 K): δ = 8.97 (s, 1H, Br-C_5H_4N), 8.93 (d, J_{HH} = 4.0 Hz, 1H, Br-C_5H_4N), 7.80 (d, J_{HH} = 7.6 Hz, 2H, $H^{3,5}$ C_5H_3N), 7.61 (t, J_{HH} = 7.6 Hz, 1H, H^4 C_5H_3N), 7.38 (m, 1H, Br-C_5H_4N), 6.94 (m, 10H, Ph), 6.45 (m, 1H, Br-C_5H_4N), 5.29 (m, 2H, OCH_2), 5.17 (m, 2H, C*H*Ph), 4.55 (m, 2H, OCH_2) ppm. $^{13}C\{^1H\}$ NMR (100.62 MHz, $CDCl_3$, 298 K): δ = 167.9 (s, OCN), 155.7 (s, CH Br-C_5H_4N), 153.4 (s, CH Br-C_5H_4N), 152.0 (s, $C^{2,6}$ C_5H_3N), 137.4 (C^{ipso} Ph), 137.1 (s, CH Br-C_5H_4N), 128.3 (br s, C^4 C_5H_3N, Ph), 123.3 (s, $C^{3,5}$ C_5H_3N), 122.8 (s, CH Br-C_5H_4N), 119.4 (s, C Br-C_5H_4N), 78.4 (s, OCH_2), 69.1 (s, *C*HPh) ppm.

Complex **5b**: Yield 58% (19 mg, 0.029 mmol). Color: dark purple. Anal. Calc. for $C_{32}H_{26}Cl_2N_4O_2Ru$ (670.56): C, 57.32; H, 3.91; N, 8.36. Found: C, 57.33; H, 3.92; N, 7.98. MS-ESI: *m/z* = 670.10 ($[RuCl_2(C_9H_7N)$(Ph-pybox)$]^+$, 100%). ^1H NMR (400.13 MHz, $CDCl_3$, 298 K): δ = 9.31 (m, 1H, C_9H_7N), 8.58 (m, 1H, C_9H_7N), 7.99 (d, J_{HH} = 7.2 Hz, 2H, $H^{3,5}$ C_5H_3N), 7.83 (m, 3H, H^4 C_5H_3N, Ph), 7.73-7.59 (m, 13H, C_9H_7N, Ph), 5.38-5.21 (m, 3H, OCH_2, C*H*Ph), 5.14 (m, 1H, C*H*Ph), 4.56 (m, 2H, OCH_2) ppm. $^{13}C\{^1H\}$ NMR (100.62 MHz, $CDCl_3$, 298 K): δ = 168.0 (s, OCN), 158.6 (s, CH C_9H_7N), 152.0 (s, $C^{2,6}$ C_5H_3N), 147.5, 137.6 (2*s*, CH C_9H_7N), 134.3, 130.4 (2*s*, C C_9H_7N), 128.2-127.5 (CH C_9H_7N, C^4 C_5H_3N, Ph), 126.2, 125.6 (2*s*, CH C_9H_7N), 123.4, 123.3 (2*s*, $C^{3,5}$ C_5H_3N), 118.6 (s, CH C_9H_7N), 78.5, 78.4 (2*s*, OCH_2), 69.1 (s, *C*HPh) ppm.

Complex **6b**: Yield 81% (25 mg, 0.040 mmol). Color: dark purple. Anal. Calc. for $C_{27}H_{23}Cl_2N_5O_2Ru$ (621.48): C, 52.18; H, 3.73; N, 11.27. Found: C, 52.66; H, 4.10; N, 10.71. ^1H NMR (400.13 MHz, $CDCl_3$, 298 K): δ = 8.69 (s, 2H, $C_4H_4N_2$), 7.82 (d, J_{HH} = 7.8 Hz, 2H, $H^{3,5}$ C_5H_3N), 7.74 (s, 2H, $C_4H_4N_2$), 7.66 (t, J_{HH} = 7.8 Hz, 1H, H^4 C_5H_3N), 7.23-7.14 (m, 10H, Ph), 5.25 (dd, J_{HH} = 11.2 Hz, J_{HH} = 8.8 Hz, 2H, OCH_2), 5.08 (pt, J_{HH} = 11.2 Hz, 2H, C*H*Ph), 4.60 (dd, J_{HH} = 11.2 Hz, J_{HH} = 8.8 Hz, 2H, OCH_2) ppm. $^{13}C\{^1H\}$ NMR (100.62 MHz, $CDCl_3$, 298 K): δ = 167.5 (s, OCN), 151.3 (s, $C^{2,6}$ C_5H_3N), 149.9 (s, $C_4H_4N_2$), 143.0 (s, $C_4H_4N_2$), 137.1 (s, C^{ipso} Ph), 129.2 (s, C^4 C_5H_3N), 128.6 (s, Ph), 123.3 (s, $C^{3,5}$ C_5H_3N), 78.4 (s, OCH_2), 69.3 (s, *C*HPh) ppm.

Complex **7b**: Yield 77% (24 mg, 0.039 mmol). Color: dark purple. Anal. Calc. for $C_{27}H_{25}Cl_2N_5O_2Ru$ (623.50): C, 52.01; H, 4.04; N, 11.23. Found: C, 51.66; H, 4.16; N, 11.06. ^1H NMR (400.13 MHz, $CDCl_3$, 298 K): δ = 7.74 (d, J_{HH} = 7.8 Hz, 2H, $H^{3,5}$ C_5H_3N), 7.50 (t, J_{HH} = 7.8 Hz, 1H, H^4 C_5H_3N), 7.22 (m, 10H, Ph), 6.97 (s, 1H, NCHCHN), 6.80 (s, 1H, NCHCHN), 6.34 (s, 1H, NCHN), 5.21 (pt, J_{HH} = 10.9 Hz, 2H, OCH_2), 5.00 (pt, J_{HH} = 10.9 Hz, 2H, C*H*Ph), 4.57 (pt, J_{HH} = 10.9 Hz, 2H, OCH_2), 3.31 (s, 3H, NCH_3) ppm. $^{13}C\{^1H\}$ NMR (100.62 MHz, $CDCl_3$, 298 K): δ = 168.2 (s, OCN), 152.3 (s, $C^{2,6}$ C_5H_3N), 140.7 (s, NCHCHN), 138.3 (s, C^{ipso} Ph), 132.1 (s, NCHCHN), 128.7, 128.1, 127.7 (3 s, Ph), 125.5 (s, C^4 C_5H_3N), 123.3 (s, $C^{3,5}$ C_5H_3N), 118.0 (s, NCHN), 78.4 (s, OCH_2), 69.0 (s, *C*HPh), 33.7 (s, NCH_3) ppm.

Complex **8b**: Yield 75% (26 mg, 0.038 mmol). Color: dark purple. Anal. Calc. for $C_{33}H_{29}Cl_2N_5O_2Ru$ (699.60): C, 56.66; H, 4.18; N, 10.01. Found: C, 56.65; H, 4.39; N, 10.14. ^1H NMR (400.13 MHz, CD_2Cl_2, 298 K): δ = 7.82 (d, J_{HH} = 7.6 Hz, 2H, $H^{3,5}$ C_5H_3N), 7.55 (m, 1H, H^4 C_5H_3N), 7.42-7.05 (m, 16H, Ph, NCHCHN), 6.96 (s, 1H, NCHCHN), 6.42 (s, 1H, NCHN), 5.27 (pt, J_{HH} = 9.2 Hz, 2H, OCH_2), 5.15 (s, 1H, NCH_2), 5.06 (m, 2H, C*H*Ph), 4.79 (s, 1H, NCH_2), 4.57 (pt, J_{HH} = 9.2 Hz, 2H, OCH_2) ppm. $^{13}C\{^1H\}$ NMR (100.62 MHz, CD_2Cl_2, 298 K): δ = 168.1 (s, OCN), 152.2 (s, $C^{2,6}$ C_5H_3N), 140.1 (s, NCHCHN), 138.4 (s, C^{ipso} Ph), 132.0 (s, NCHCHN), 128.9-127.2 (Ph), 125.1 (s, C^4 C_5H_3N), 122.9 (s, $C^{3,5}$ C_5H_3N), 117.4 (s, NCHN), 78.5 (s, OCH_2), 68.9 (s, *C*HPh), 50.9 (s, NCH_2) ppm.

Complex **9b**: Yield 76% (23 mg, 0.038 mmol). Color: dark pink. Anal. Calc. for $C_{26}H_{23}Cl_2N_5O_2Ru$ (609.47): C, 51.24; H, 3.80; N, 11.49. Found: C, 51.19; H, 3.69; N, 11.36. ^1H NMR (400.13 MHz, $CDCl_3$, 298 K): δ = 10.89 (s, 1H, NH), 7.78 (d, J_{HH} = 8.0 Hz, 2H, $H^{3,5}$ C_5H_3N), 7.57 (t, J_{HH} = 8.0 Hz, 1H, H^4 C_5H_3N), 7.47 (s, 1H, CH $C_3H_4N_2$), 7.18 (m, 6H, Ph), 7.10 (m, 4H, Ph), 7.00 (s, 1H, CH $C_3H_4N_2$), 5.94 (s, 1H, CH $C_3H_4N_2$), 5.22 (pt, J_{HH} = 9.6 Hz, 2H, OCH_2), 4.95 (pt, J_{HH} = 9.6 Hz, 2H, C*H*Ph), 4.64 (pt, J_{HH} = 9.6 Hz, 2H, OCH_2) ppm. $^{13}C\{^1H\}$ NMR (100.62 MHz, $CDCl_3$, 298 K): δ = 167.6 (s, OCN), 152.5 (s, $C^{2,6}$ C_5H_3N), 141.6 (s, $C_3H_4N_2$), 137.4 (s, C^{ipso} Ph), 128.5, 128.2, 127.9 (3 s, Ph), 127.7 (s, $C_3H_4N_2$), 127.0 (s, C^4 C_5H_3N), 123.2 (s, $C^{3,5}$ C_5H_3N), 105.2 (s, CH $C_3H_4N_2$), 78.4 (s, OCH_2), 69.0 (s, *C*HPh) ppm.

Complex **10b**: Yield 80% (25 mg, 0.040 mmol). Color: dark pink. Anal. Calc. for $C_{27}H_{25}Cl_2N_5O_2Ru{\cdot}0.5Et_2O$ (660.56): C, 52.73; H, 4.58; N, 10.60. Found: C, 52.43; H, 5.03; N, 10.79. ^1H NMR (400.13 MHz, $CDCl_3$, 298 K): δ = 10.41 (s, 1H, NH), 7.77 (d, J_{HH} = 7.6 Hz, 2H, $H^{3,5}$ C_5H_3N), 7.55 (m, 1H, H^4 C_5H_3N), 7.24-6.93 (m, 11H, CH $C_4H_6N_2$, Ph), 5.65 (s, 1H, CH $C_4H_6N_2$), 5.22 (pt, J_{HH} = 10.0 Hz, 2H, OCH_2), 5.12 (pt, J_{HH} = 10.0 Hz, 1H, C*H*Ph), 4.96 (pt, J_{HH} = 10.0 Hz, 1H, C*H*Ph), 4.64 (pt, J_{HH} = 10.0 Hz, 2H, OCH_2), 1.97 (s, 3H, CH_3) ppm. $^{13}C\{^1H\}$ NMR (100.62 MHz, $CDCl_3$, 298 K): δ = 167.7 (s, OCN), 152.7 (s, $C^{2,6}$ C_5H_3N), 142.6 (s, CH $C_4H_6N_2$), 137.9, 137.6 (2*s*, *C*CH$_3$, C^{ipso} Ph), 128.6-127.8 (Ph), 126.8 (s, C^4 C_5H_3N), 123.3 (s, $C^{3,5}$ C_5H_3N), 104.8 (s, CH $C_4H_6N_2$), 78.4 (s, OCH_2), 69.0 (s, *C*HPh), 10.8 (s, CH_3) ppm.

Complex **11b**: Yield 83% (25 mg, 0.042 mmol). Color: dark pink.

Anal. Calc. for $C_{25}H_{22}Cl_2N_6O_2Ru$ (610.46): C, 49.19; H, 3.63; N, 13.77. Found: C, 49.56; H, 3.89; N, 14.09. ^{1}H NMR (400.13 MHz, CD_2Cl_2, 298 K): δ = 11.85 (s, 1H, NH), 7.86 (d, J_{HH} = 7.6 Hz, 2H, $H^{3,5}$ C_5H_3N), 7.85 (s, 1H, CH $C_2H_3N_3$), 7.75 (s, 1H, CH $C_2H_3N_3$), 7.67 (t, J_{HH} = 7.6 Hz, 1H, H^4 C_5H_3N), 7.29-7.13 (m, 10H, Ph), 5.30 (dd, J_{HH} = 10.6 Hz, J_{HH} = 8.8 Hz, 2H, OCH_2), 4.98 (pt, J_{HH} = 10.6 Hz, 2H, C*H*Ph), 4.69 (dd, J_{HH} = 10.6 Hz, J_{HH} = 8.8 Hz, 2H, OCH_2) ppm. ^{13}C{^{1}H} NMR (100.62 MHz, CD_2Cl_2, 298 K): δ = 167.4 (s, OCN), 152.7 (s, $C^{2,6}$ C_5H_3N), 152.0, 142.0 (2*s*, $C_2H_3N_3$), 137.4 (s, C^{ipso} Ph), 128.5-127.5 (Ph), 126.8 (s, C^4 C_5H_3N), 123.1 (s, $C^{3,5}$ C_5H_3N), 78.5 (s, OCH_2), 69.0 (s, *C*HPh) ppm.

*4.4. Synthesis of complexes trans-[OsCl$_2$(L){(S,S)-^{i}Pr-pybox}] (L = py (**12**), 3-Br-py (**13**), 3-CN-py (**14**), 3-MeO-py (**15**), 3-NO$_2$-py (**16**), 4-CN-py (**17**), 4-MeO-py (**18**), isoquinoline (**19**), 1-methylimidazole (**20**), 1-benzylimidazole (**21**), pyrazole (**22**))*

To a solution of complex *trans*-[$OsCl_2(\eta^2$-$C_2H_4)${(*S*,*S*)-^{i}Pr-pybox}] (**2**) (0.100 g, 0.17 mmol) in toluene (25 mL) the corresponding ligand (0.26 mmol) was added and the mixture heated under reflux during 90 min. The solvent was then evaporated under reduced pressure and hexane (20 mL) was added yielding a solid that was washed with hexane (3 × 5 mL) and vacuum-dried.

Complex **12**: Yield: 83% (0.090 g). Color: dark pink. Exact mass for $C_{22}H_{28}Cl_2N_4O_2Os$ (642.12). MS-ESI: *m/z* = 642.1 ([$OsCl_2(C_5H_5N)$(^{i}Pr-pybox)]$^+$, 100%). ^{1}H NMR (400.13 MHz, CD_2Cl_2, 298 K): δ = 9.57 (m, 2H, C_5H_5N), 7.79 (t, J_{HH} = 7.4 Hz, 1H, C_5H_5N), 7.48 (m, 2H, C_5H_5N), 6.61 (m, 2H, $H^{3,5}$ C_5H_3N), 6.09 (t, J_{HH} = 7.6 Hz, 1H, H^4 C_5H_3N), 5.23 (m, 2H, OCH_2), 5.03 (m, 2H, OCH_2), 4.20 (m, 2H, C*H*^{i}Pr), 1.72 (m, 2H, C*H*Me$_2$), 0.83 (d, J_{HH} = 6.6 Hz, 6H, CH*Me*$_2$), 0.72 (d, J_{HH} = 6.6 Hz, 6H, CH*Me*$_2$) ppm. ^{13}C{^{1}H} NMR (100.62 MHz, CD_2Cl_2, 298 K): δ = 175.2 (s, OCN), 155.3 (s, C_5H_5N), 145.4 (s, $C^{2,6}$ C_5H_3N), 135.5, 124.2 (2 s, C_5H_5N), 121.9 (s, $C^{3,5}$ C_5H_3N), 120.7 (s, C^4 C_3H_5N), 70.9 (s, OCH_2), 70.7 (s, *C*H^{i}Pr), 29.8 (s, *C*HMe$_2$), 18.9, 15.4 (2*s*, CH*Me*$_2$) ppm.

Complex **13**: Yield: 95% (0.121 g). Color: dark pink. Exact mass for $C_{22}H_{27}BrCl_2N_4O_2Os$ (720.03). MS-ESI: *m/z* = 720.0 ([$OsCl_2(C_5H_4NBr)$(^{i}Pr-pybox)]$^+$, 100%). ^{1}H NMR (400.13 MHz, CD_2Cl_2, 298 K): δ = 9.73 (m, 1H, Br-C_5H_4N), 9.53 (m, 1H, Br-C_5H_4N), 7.94 (m, 1H, Br-C_5H_4N), 7.35 (m, 1H, Br-C_5H_4N), 6.68 (m, 2H, $H^{3,5}$ C_5H_3N), 6.16 (m, 1H, H^4 C_5H_3N), 5.22 (m, 2H, OCH_2), 5.01 (m, 2H, OCH_2), 4.19 (m, 2H, C*H*^{i}Pr), 1.71 (m, 2H, C*H*Me$_2$), 0.87 (m, 6H, CH*Me*$_2$), 0.73 (m, 6H, CH*Me*$_2$) ppm. ^{13}C{^{1}H} NMR (100.62 MHz, CD_2Cl_2, 298 K): δ = 175.3 (s, OCN), 156.3, 153.8 (2*s*, CH Br-C_5H_4N), 145.4 (s, $C^{2,6}$ C_5H_3N), 137.9 (s, CH Br-C_5H_4N), 125.4 (s, C Br-C_5H_4N), 124.9 (s, CH Br-C_5H_4N), 121.9 (s, $C^{3,5}$ C_5H_3N), 120.1 (s, C^4 C_3H_5N), 70.9 (s, OCH_2), 70.3 (s, *C*H^{i}Pr), 29.9 (s, *C*HMe$_2$), 19.2, 15.4 (2*s*, CH*Me*$_2$) ppm.

Complex **14**: Yield: 86% (0.097 g). Color: dark purple. Exact mass for $C_{23}H_{27}Cl_2N_5O_2Os$ (667.12) MS-ESI: *m/z* = 667.1 ([$OsCl_2(C_6H_4N_2)$(^{i}Pr-pybox)]$^+$, 100%). IR (KBr, cm^{-1}): 2234 (m) ν(C≡N). ^{1}H NMR (300.13 MHz, CD_2Cl_2, 298 K): δ = 10.07 (m, 1H, CN-C_5H_4N), 9.99 (m, 1H, CN-C_5H_4N), 8.07 (m, 1H, CN-C_5H_4N), 7.59 (m, 1H, CN-C_5H_4N), 6.97 (m, 2H, $H^{3,5}$ C_5H_3N), 6.22 (m, 1H, H^4 C_5H_3N), 5.19 (m, 2H, OCH_2), 5.00 (m, 2H, OCH_2), 4.18 (m, 2H, C*H*^{i}Pr), 1.66 (m, 2H, C*H*Me$_2$), 0.86 (d, J_{HH} = 6.6 Hz, 6H, CH*Me*$_2$), 0.72 (d, J_{HH} = 6.6 Hz, 6H, CH*Me*$_2$) ppm. ^{13}C{^{1}H} NMR (100.62 MHz, CD_2Cl_2, 298 K): δ = 174.8 (s, OCN), 158.7, 157.6 (2*s*, CH CN-C_5H_4N), 145.8 (s, $C^{2,6}$ C_5H_3N), 137.6, 124.4 (2*s*, CH CN-C_5H_4N), 123.1 (s, C^4 C_3H_5N), 121.9, 121.7 (2*s*, $C^{3,5}$ C_5H_3N), 115.6 (s, C CN-C_5H_4N), 110.8 (s, CN), 71.2 (s, OCH_2), 70.6 (s, *C*H^{i}Pr), 29.3 (s, *C*HMe$_2$), 19.1, 15.4 (2*s*, CH*Me*$_2$) ppm.

Complex **15**: Yield: 74% (0.085 g). Color: dark pink. Exact mass for $C_{23}H_{30}Cl_2N_4O_3Os$ (672.13). MS-ESI: *m/z* = 672.0 ([$OsCl_2(C_6H_7NO)$(^{i}Pr-pybox)]$^+$, 100%). ^{1}H NMR (400.13 MHz, CD_2Cl_2, 298 K): δ = 9.20 (m, 1H, MeO-C_5H_4N), 9.05 (m, 1H, MeO-C_5H_4N), 7.30 (m, 2H, MeO-C_5H_4N), 6.28 (m, 2H, $H^{3,5}$ C_5H_3N), 6.13 (m, 1H, H^4 C_5H_3N), 5.31 (m, 2H, OCH_2), 5.04 (m, 2H, OCH_2), 4.18 (m, 2H, C*H*^{i}Pr), 3.95 (s, 3H, OCH_3), 1.70 (m, 2H, C*H*Me$_2$), 0.83 (m, 6H, CH*Me*$_2$), 0.75 (m, 6H CH*Me*$_2$) ppm. ^{13}C{^{1}H} NMR (100.62 MHz, CD_2Cl_2, 298 K): δ = 177.4 (s, OCN), 155.8 (s, C MeO-C_5H_4N), 147.4 (s, CH MeO-C_5H_4N), 144.8 (s, $C^{2,6}$ C_5H_3N), 143.0, 124.1 (2*s*, CH MeO-C_5H_4N), 123.4 (s, $C^{3,5}$ C_5H_3N), 120.4, 120.1 (2*s*, C^4 C_3H_5N, CH MeO-C_5H_4N), 70.7 (s, OCH_2, *C*H^{i}Pr), 55.8 (s, OCH_3), 29.8 (s, *C*HMe$_2$), 19.2, 15.6 (2*s*, CH*Me*$_2$) ppm.

Complex **16**: Yield: 75% (0.087 g). Color: dark purple. Exact mass for $C_{22}H_{27}Cl_2N_5O_4Os$ (687.11). MS-ESI: *m/z* = 687.0 ([$OsCl_2(C_5H_4N_2O_2)$(^{i}Pr-pybox)]$^+$, 99%). IR (KBr, cm^{-1}): 1531 (m), 1261 (m) ν(NO$_2$). ^{1}H NMR (400.13 MHz, CD_2Cl_2, 298 K): δ = 10.57 (s, 1H, NO_2-C_5H_4N), 10.07 (m, 1H, NO_2-C_5H_4N), 8.58 (m, 1H, NO_2-C_5H_4N), 7.65 (m, 1H, NO_2-C_5H_4N), 6.96 (d, J_{HH} = 7.2 Hz, 2H, $H^{3,5}$ C_5H_3N), 6.26 (t, J_{HH} = 7.2 Hz, 1H, H^4 C_5H_3N), 5.20 (m, 2H, OCH_2), 5.03 (m, 2H, OCH_2), 4.22 (m, 2H, C*H*^{i}Pr), 1.70 (m, 2H, C*H*Me$_2$), 0.84 (d, J_{HH} = 6.4 Hz, 6H, CH*Me*$_2$), 0.72 (d, J_{HH} = 6.4 Hz, 6H CH*Me*$_2$) ppm. ^{13}C{^{1}H} NMR (100.62 MHz, CD_2Cl_2, 298 K): δ = 173.9 (s, OCN), 160.6, 151.3 (2*s*, CH NO_2-C_5H_4N), 146.3 (s, $C^{2,6}$ C_5H_3N), 144.9 (s, C NO_2-C_5H_4N), 129.7, 124.4 (2*s*, CH NO_2-C_5H_4N), 123.6 (s, C^4 C_3H_5N), 121.3 (s, $C^{3,5}$ C_5H_3N), 71.3 (s, OCH_2), 70.7 (s, *C*H^{i}Pr), 30.1 (s, *C*HMe$_2$), 19.1, 15.3 (2*s*, CH*Me*$_2$) ppm.

Complex **17**: Yield: 89% (0.101 g). Color: dark purple. Exact mass for $C_{23}H_{27}Cl_2N_5O_2Os$ (667.12). MS-ESI: *m/z* = 667.1 ([$OsCl_2(C_6H_4N_2)$(^{i}Pr-pybox)]$^+$, 100%). IR (KBr, cm^{-1}): 2234 (m) ν(C≡N). ^{1}H NMR (300.13 MHz, CD_2Cl_2, 298 K): δ = 9.94 (d, J_{HH} = 6.0 Hz, 2H, CN-C_5H_4N), 7.60 (d, J_{HH} = 6.0 Hz, 2H, CN-C_5H_4N), 6.96 (d, J_{HH} = 9.0 Hz, 2H, $H^{3,5}$ C_5H_3N), 6.28 (t, J_{HH} = 9.0 Hz, 1H, H^4 C_5H_3N), 5.18 (m, 2H, OCH_2), 4.98 (m, 2H, OCH_2), 4.18 (m, 2H, C*H*^{i}Pr), 1.65 (m, 2H, C*H*Me$_2$), 0.84 (d, J_{HH} = 6.0 Hz, 6H, CH*Me*$_2$), 0.71 (d, J_{HH} = 6.0 Hz, 6H, CH*Me*$_2$) ppm. ^{13}C{^{1}H} NMR (100.62 MHz, CD_2Cl_2, 298 K): δ = 173.8 (s, OCN), 156.6 (s, CH CN-C_5H_4N), 146.1 (s, $C^{2,6}$ C_5H_3N), 125.5 (s, CH CN-C_5H_4N), 124.7 (s, C^4 C_3H_5N), 121.1 (s, $C^{3,5}$ C_5H_3N), 117.5, 116.8 (2*s*, C CN-C_5H_4N, CN), 71.3 (s, OCH_2), 70.6 (s, *C*H^{i}Pr), 30.0 (s, *C*HMe$_2$), 19.0, 15.2 (2*s*, CH*Me*$_2$) ppm.

Complex **18**: Yield: 93% (0.106 g). Color: dark pink. Exact mass for $C_{23}H_{30}Cl_2N_4O_3Os$ (672.13). MS-ESI: *m/z* = 672.0 ([$OsCl_2(C_6H_7NO)$(^{i}Pr-pybox)]$^+$, 100%). ^{1}H NMR (400.13 MHz, CD_2Cl_2, 298 K): δ = 9.28 (m, 2H, MeO-C_5H_4N), 7.01 (m, 2H, MeO-C_5H_4N), 6.40 (m, 2H, $H^{3,5}$ C_5H_3N), 6.06 (m, 1H, H^4 C_5H_3N), 5.27 (m, 2H, OCH_2), 5.05 (m, 2H, OCH_2), 4.18 (m, 2H, C*H*^{i}Pr), 4.03 (s, 3H, OCH_3), 1.75 (m, 2H, C*H*Me$_2$), 0.86 (m, 6H, CH*Me*$_2$), 0.74 (m, 6H CH*Me*$_2$) ppm. ^{13}C{^{1}H} NMR (100.62 MHz, CD_2Cl_2, 298 K): δ = 177.7 (s, OCN), 165.6 (s, C MeO-C_5H_4N), 155.6 (s, CH MeO-C_5H_4N), 144.8 (s, $C^{2,6}$ C_5H_3N), 122.0 (s, $C^{3,5}$ C_5H_3N), 119.1 (s, C^4 C_3H_5N), 110.4 (s, CH MeO-C_5H_4N), 70.6 (s, OCH_2, *C*H^{i}Pr), 55.8 (s, OCH_3), 29.8 (s, *C*HMe$_2$), 19.3, 15.6 (2*s*, CH*Me*$_2$) ppm.

Complex **19**: Yield: 91% (0.107 g). Color: dark pink. Exact mass for $C_{26}H_{30}Cl_2N_4O_2Os$ (692.14). MS-ESI: *m/z* = 692.2 ([$OsCl_2(C_9H_7N)$(^{i}Pr-pybox)]$^+$, 100%). ^{1}H NMR (400.13 MHz, CD_2Cl_2, 298 K): δ = 10.16 (m, 1H, C_9H_7N), 9.44 (m, 1H, C_9H_7N), 8.06 (m, 2H, C_9H_7N), 7.79 (m, 3H, C_9H_7N), 6.59 (m, 2H, $H^{3,5}$ C_5H_3N), 6.12 (m, 1H, H^4 C_5H_3N), 5.27 (m, 2H, OCH_2), 5.04 (m, 2H, OCH_2), 4.30 (m, 2H, C*H*^{i}Pr), 1.88 (m, 2H, C*H*Me$_2$), 0.76 (m, 6H, CH*Me*$_2$), 0.69 (m, 6H, CH*Me*$_2$) ppm. ^{13}C{^{1}H} NMR (100.62 MHz, CD_2Cl_2, 298 K): δ = 176.6 (s, OCN), 157.7, 148.3 (2 s, CH C_9H_7N), 145.7 (s, $C^{2,6}$ C_5H_3N), 135.2 (s, C C_9H_7N), 131.3 (s, CH C_9H_7N), 129.1-126.3 (C_9H_7N), 121.9-120.7 (s, $C^{3,4,5}$ C_5H_3N, C_9H_7N), 71.0 (s, OCH_2), 70.8 (s, *C*H^{i}Pr), 29.8 (s, *C*HMe$_2$), 19.2, 15.4 (2*s*, CH*Me*$_2$) ppm.

Complex **20**: Yield: 93% (0.102 g). Color: brick red. Exact mass for $C_{21}H_{29}Cl_2N_5O_2Os$ (645.13). MS-ESI: *m/z* = 645.1 ([$OsCl_2(C_4H_6N_2)$(^{i}Pr-pybox)]$^+$, 100%). ^{1}H NMR (400.13 MHz, CD_2Cl_2, 298 K): δ = 7.79 (s, 1H, NCHCHN), 7.39 (s, 1H, NCHCHN), 6.83 (m, 2H, $H^{3,5}$ C_5H_3N), 6.15 (m, 1H, H^4 C_5H_3N), 5.58 (m, 2H, OCH_2), 5.16 (m, 2H, OCH_2), 5.00 (br s, 1H, NCHN), 4.09 (m, 2H, C*H*^{i}Pr), 3.78 (s, 3H, NCH_3), 1.62 (m, 2H, C*H*Me$_2$), 0.84-0.80 (m, 12H, CH*Me*$_2$) ppm. ^{13}C{^{1}H} NMR (100.62 MHz, CD_2Cl_2, 298 K): δ = 176.8 (s, OCN), 141.6 (s, $C^{2,6}$ C_5H_3N), 138.3 (s, NCHCHN), 130.4 (s, NCHCHN, NCHN), 120.2 (s, $C^{3,5}$ C_5H_3N), 116.1 (s, C^4 C_3H_5N), 71.5 (s, *C*H^{i}Pr), 70.3 (s, OCH_2), 34.4 (s, NCH_3), 29.7 (s, *C*HMe$_2$), 19.7, 16.6 (2*s*, CH*Me*$_2$) ppm.

Complex **21**: Yield: 89% (0.109 g). Color: brick red. Exact mass for

$C_{27}H_{33}Cl_2N_5O_2Os$ (721.16). MS-ESI: *m/z* = 721.1 ([$OsCl_2(C_{10}H_{10}N_2)$ (^{i}Pr-pybox)]$^+$, 100%). ^{1}H NMR (400.13 MHz, CD_2Cl_2, 298 K): δ = 8.49 (s, 1H, NCHCHN), 8.02 (s, 1H, NCHCHN), 7.42 (m, 3H, Ph), 7.28 (m, 2H, Ph), 7.18 (s, 1H, NCHN), 6.50 (m, 2H, $H^{3,5}$ C_5H_3N), 5.94 (m, 1H, H^4 C_5H_3N), 5.36 (m, 1H, NCH_2), 5.15 (m, 3H, NCH_2, OCH_2), 5.01 (m, 2H, OCH_2), 4.07 (m, 2H, C*H*^{i}Pr), 1.86 (m, 2H, C*H*Me_2), 0.83 (d, J_{HH} = 6.6 Hz, 6H, CH*Me*$_2$), 0.75 (d, J_{HH} = 6.6 Hz, 6H, CH*Me*$_2$) ppm. ^{13}C{^{1}H} NMR (100.62 MHz, CD_2Cl_2, 298 K): δ = 176.9 (s, OCN), 145.4 (s, $C^{2,6}$ C_5H_3N), 139.6 (s, NCHCHN), 137.6 (s, C^{ipso} Ph), 132.1 (s, NCHCHN), 129.1-127.2 (Ph), 122.6 (s, $C^{3,5}$ C_5H_3N), 119.6 (s, NCHN), 117.7 (s, C^4 C_3H_5N), 72.2 (s, C*H*^{i}Pr), 70.8 (s, OCH_2), 51.7 (s, NCH_2), 29.5 (s, C*H*Me_2), 19.3, 15.5 (2*s*, CH*Me*$_2$) ppm.

Complex **22**: Yield: 74% (0.079 g). Color: brick red. Exact mass for $C_{20}H_{27}Cl_2N_5O_2Os$ (631.12). MS-ESI: *m/z* = 631.1 ([$OsCl_2(C_3H_4N_2)$(^{i}Pr-pybox)]$^+$, 100%). ^{1}H NMR (400.13 MHz, CD_2Cl_2, 298 K): δ = 11.96 (br s, 1H, NH), 8.00 (m, 1H, CH $C_3H_4N_2$), 7.45 (m, 2H, $H^{3,5}$ C_5H_3N), 6.40 (m, 1H, CH $C_3H_4N_2$), 6.18 (m, 2H, CH $C_3H_4N_2$, H^4 C_5H_3N), 5.53 (m, 2H, OCH_2), 5.09 (m, 2H, OCH_2), 4.03 (m, 2H, C*H*^{i}Pr), 1.52 (m, 2H, C*H*Me_2), 0.79 (m, 12H, CH*Me*$_2$) ppm. ^{13}C{^{1}H} NMR (100.62 MHz, CD_2Cl_2, 298 K): δ = 169.1 (s, OCN), 153.9 (s, $C^{2,6}$ C_5H_3N), 143.1, 137.5 (2 s, $C_3H_4N_2$), 129.2 (s, $C^{3,5}$ C_5H_3N), 118.1 (s, C^4 C_3H_5N), 105.6 (s, $C_3H_4N_2$), 71.9 (s, C*H*^{i}Pr), 70.1 (s, OCH_2), 29.3 (s, C*H*Me_2), 19.5, 16.4 (2*s*, CH*Me*$_2$) ppm.

4.5. Synthesis of the dinuclear complexes [{$RuCl_2$(R-pybox)}$_2$(μ-N,N-$C_4H_4N_2$)] (R = (S,S)-^{i}Pr **(23a)**, (R,R)-Ph **(23b))**

Method A: To a solution of complex *trans*-[$RuCl_2(\eta^2$-$C_2H_4)$(R-pybox)] (R = (*S,S*)-^{i}Pr (**1a**), (*R,R*)-Ph (**1b**)) (0.125 mmol) in dichloromethane (10 mL) pyrazine (5 mg, 0.062 mmol) was added and the mixture heated under reflux for 5.5 h (for **23a**) or at 55 °C (sealed tube) for 6.5 h (for **23b**). The solvent was then evaporated under reduced pressure and diethyl ether (20 mL) was added yielding a solid that was washed with diethyl ether (3 x 5 mL) and vacuum-dried.

Method B: A mixture of complexes **1a** (0.06 mmol) and **6a** (0.06 mmol) in dichloromethane (10 mL) was heated under reflux for 5.5 h. The solvent was then evaporated under reduced pressure and diethyl ether (30 mL) was added yielding a solid (**23a**) that was washed with diethyl ether (3 x 5 mL) and vacuum-dried. Complex **23b** was similarly synthesized by reaction of equimolecular amounts of **1b** and **6b** in dichloromethane (sealed tube, 55 °C, 5.5 h).

Complex **23a**: Yield 88% (54 mg, 0.053 mmol, *method A*), 86% (53 mg, 0.051 mmol, *method B*). Color: dark blue. Exact mass for $C_{38}H_{50}Cl_4N_8O_4Ru_2$ (1026.08). MS-ESI: *m/z* = 1025.1 [$Ru_2Cl_4(C_4H_4N_2)$ (^{i}Pr-pybox)$_2$-1]$^+$ (100%). ^{1}H NMR (400.13 MHz, $CDCl_3$, 298 K): δ = 9.95 (s, 4H, CH $C_4H_4N_2$), 7.75 (m, 4H, $H^{3,5}$ C_5H_3N), 7.63 (m, 2H, H^4 C_5H_3N), 4.90 (m, 4H, OCH_2), 4.75 (m, 4H, OCH_2), 4.23 (m, 4H, C*H*^{i}Pr), 1.72 (m, 2H, C*H*Me_2), 1.59 (m, 2H, C*H*Me_2), 0.84 (d, J_{HH} = 6.8 Hz, 8H, CH*Me*$_2$), 0.77 (d, J_{HH} = 6.8 Hz, 12H, CH*Me*$_2$), 0.72 (d, J_{HH} = 6.8 Hz, 4H, CH*Me*$_2$) ppm. ^{13}C{^{1}H} NMR (100.62 MHz, $CDCl_3$, 298 K): δ = 165.8 (s, OCN), 150.9, 150.7 (2*s*, $C^{2,6}$ C_5H_3N), 150.1 (s, $C_4H_4N_2$), 130.2, 129.8 (2*s*, C^4 C_5H_3N), 123.1 (s, $C^{3,5}$ C_5H_3N), 72.2, 71.7 (2*s*, OCH_2), 69.0 (s, C*H*^{i}Pr), 30.4, 30.0 (2*s*, C*H*Me_2), 19.6, 19.0, 15.9, 15.5 (4*s*, CH*Me*$_2$) ppm.

Complex **23b**: Yield 89% (62 mg, 0.053 mmol, *method A*), 86% (57 mg, 0.049 mmol, *method B*). Color: dark blue. Anal. Calc. for $C_{50}H_{42}Cl_4N_8O_4Ru_2$ (1162.88): C, 51.64; H, 3.64; N, 9.64. Found: C, 51.42; H, 3.87; N, 9.31. MS-ESI: *m/z* = 1164.1 ([$Ru_2Cl_4(C_4H_4N_2)$(Ph-pybox)$_2$+1]$^+$, 100%). ^{1}H NMR (400.13 MHz, $CDCl_3$, 298 K): δ = 7.83 (d, J_{HH} = 8.0 Hz, 4H, $H^{3,5}$ C_5H_3N), 7.65 (t, J_{HH} = 8.0 Hz, 2H, H^4 C_5H_3N), 7.34-7.30 (m, 14H, Ph), 7.22 (s, 4H, CH $C_4H_4N_2$), 7.14-7.10 (m, 6H, Ph), 5.25 (pt, J_{HH} = 10.0 Hz, 4H, OCH_2), 4.95 (pt, J_{HH} = 10.0 Hz, 4H, C*H*Ph), 4.69 (pt, J_{HH} = 10.0 Hz, 4H, OCH_2) ppm. ^{13}C{^{1}H} NMR (100.62 MHz, $CDCl_3$, 298 K): δ = 167.0 (s, OCN), 151.0 (s, $C^{2,6}$ C_5H_3N), 148.0 (s, $C_4H_4N_2$), 137.0 (s, C^{ipso} Ph), 129.8-127.7 (Ph, C^4 C_5H_3N), 123.3 (s, $C^{3,5}$ C_5H_3N), 78.6 (s, OCH_2), 69.8 (s, C*H*Ph) ppm.

4.6. Synthesis of complex [($OsCl_2$[(S,S)-^{i}Pr-pybox])$_2$(μ-N,N-$C_6H_4N_2$)] **(24)**

To a solution of complex *trans*-[$OsCl_2(\eta^2$-$C_2H_4)$[(*S,S*)-^{i}Pr-pybox}] (**2**) (0.100 g, 0.17 mmol) in toluene (25 mL), pyrazine (0.020 g, 0.255 mmol) was added and the mixture heated under reflux during 80 min. The solvent was then evaporated under reduced pressure and hexane (30 mL) was added yielding a solid that was washed with hexane (3 x 5 mL) and vacuum-dried. Yield: 84% (0.086 g). Color: dark purple. Exact mass for $C_{21}H_{27}Cl_2N_5O_2Os$ (643.12). Exact mass for $C_{38}H_{50}Cl_4N_8O_4Os_2$ (1206.19). MS-ESI: *m/z* = 643.1 ([$OsCl_2(C_4H_4N_2)$ (^{i}Pr-pybox)]$^+$, 100%). ^{1}H NMR (400.13 MHz, CD_2Cl_2, 298 K): δ = 9.75 (m, 1H, $C_4H_4N_2$), 9.54 (m, 2H, $C_4H_4N_2$), 8.57 (m, 1H, $C_4H_4N_2$), 6.91 (m, 4H, $H^{3,5}$ C_5H_3N), 6.35 (m, 2H, H^4 C_5H_3N), 5.25 (pt, J_{HH} = 9.4 Hz, 2H, OCH_2), 5.18 (pt, J_{HH} = 9.4 Hz, 2H, OCH_2), 5.00 (m, 4H, OCH_2), 4.27 (m, 2H, C*H*^{i}Pr), 4.20 (m, 2H, C*H*^{i}Pr), 1.86 (m, 2H, C*H*Me_2), 1.68 (m, 2H, C*H*Me_2), 0.91-0.79 (m, 24H, CH*Me*$_2$) ppm. ^{13}C{^{1}H} NMR (100.62 MHz, CD_2Cl_2, 298 K): δ = 173.7, 173.4 (2 s, OCN), 149.9, 149.3 (2 s, $C_4H_4N_2$), 145.9 (s, $C^{2,6}$ C_5H_3N), 145.3 (s, $C_4H_4N_2$), 125.8, 124.7 (2 s, C^4 C_3H_5N), 121.2, 120.9 (2 s, $C^{3,5}$ C_5H_3N), 71.8, 71.3 (2 s, OCH_2), 70.7 (s, C*H*^{i}Pr), 30.4, 30.0 (2 s, C*H*Me_2), 19.0, 18.9, 15.7, 15.2 (4*s*, CH*Me*$_2$) ppm.

4.7. General procedure for hydrogen transfer reactions

The catalyst [0.4 mol % (complexes **12**-**22**) or 0.2 mol % (dinuclear complex **24**)] and the ketone (2.5 mmol) were placed in a three-bottom Schlenk flask under dry argon atmosphere and 2-propanol (45 mL) was added. After stirring the mixture for 15 min at 82 °C, 5 ml of a 0.06 M solution of base (Cs_2CO_3) in 2-propanol (0.3 mmol) were added. The reaction was monitored by gas chromatography using an HP-6890 equipment. The corresponding alcohol and ketone were the only products detected in all cases. The conversion and *e.e.*values were determined by GC with a Supelco β-DEX 120 chiral capillary column.

4.8. X-Ray crystal structure determination of complexes **9a, 12, 23a** and **24**

Suitable crystals for X-ray diffraction analysis were obtained using liquid diff ;usion techniques. Mixtures of dichloromethane/hexane (**9a**), acetone/hexane (**12**), dichloromethane/diethyl ether (**23a**) and dichloromethane/pentane (**24**) proved effective for these complexes. The most relevant crystal and refinement data are collected in the Tables *S*8 and *S*9 (Supporting Information).

Crystallographic data of **9a** were collected at 100 K using a Bruker Smart 6000 CCD detector and Cu-Kα radiation (λ = 1.54184 Å) generated by a Incoatec microfocus source equipped with Incoatec Quazar MX optics. The software $APEX_2$ [30] was used for collecting frames of data, indexing reflections, and the determination of lattice parameters, SAINT [30] for integration of intensity of reflections, and SADABS [31] for scaling and empirical absorption correction.

The diffraction data of complexes **12**, **23a** and **24** were recorded on an Oxford Diffraction Xcalibur Nova (Agilent) single crystal diffractometer, at 150 K, using Cu-Kα radiation (λ = 1.54184 Å). Images were collected at a 62, 63 and 63 mm fixed crystal-detector distance, respectively, using the oscillation method, with 1° oscillation and variable exposure time per image. The data collection strategy was calculated with the program CrysAlis^{Pro} CCD [32]. Data reduction and cell refinement was performed with the program CrysAlis^{Pro} RED [32]. An empirical absorption correction was applied using the SCALE3 ABSPACK algorithm as implemented in the program CrysAlis^{Pro} RED [32].

The software package WINGX [33] was used for space group determination, structure solution and refinement. The structure for the complex **9a** was solved by Patterson interpretation and phase expansion using DIRDIF [34]. The structures of the complexes **12**, **23a** and **24** were solved by direct methods using SIR92 [35]. For complex **12**, the

asymmetric unit contains two formula units. In the crystal of **23a** and **24**, $1Et_2O$ and $2CH_2Cl_2$ solvent molecules, respectively, per unit formula of the complex was found.

Isotropic least-squares refinement on F^2 using SHELXL2013 [36] was performed. During the final stages of the refinements, all the positional parameters and the anisotropic temperature factors of all the non-H atoms were refined. The H atoms were geometrically located and their coordinates were refined riding on their parent atoms (except H (5 N) and H(10 N) for **9a**, which were found from different Fourier maps and included in a refinement with isotropic parameters). The maximun residual electron density was located near to heavy atoms.

The function minimized was $[\Sigma w(Fo^2 - Fc^2)/ \Sigma w(Fo^2)]^{1/2}$ where $w = 1/[\sigma^2(Fo^2) + (aP)^2 + bP]$ (a and b values are collected in the Table $S1$ y $S2$ in the Supporting Information) from counting statistics and $P = (\text{Max}\ (Fo^2, 0) + 2Fc^2)/3$.

Atomic scattering factors were taken from the International Tables for X-Ray Crystallography [37]. The crystallographic plots were made with PLATON [38] and geometrical calculations were made with PARST [39].

Acknowledgements

This work was supported by the MICINN of Spain (CTQ2011-26481). E. de *J*. thanks FICYT (Principado de Asturias, Spain) for a predoctoral fellowship (BP12-158).

Appendix A. Supplementary data

Supplementary material related to this article can be found, in the online version, at doi:https://doi.org/10.1016/j.mcat.2018.07.002.

References

[1] (a) For selected representative reviews, see: F. Schwizer, Y. Okamoto, T. Heinisch, Y. Gu, M.M. Pellizzoni, V. Lebrun, R. Reuter, V. Köhler, J.C. Lewis, T.R. Ward, Chem. Rev. 118 (2018) 142–231;
(b) P.-G. Echeverria, T. Ayad, P. Phansavath, V. Ratovelomanana, Vidal, Synthesis 48 (2016) 2523–2539;
(c) J. Ito, H. Nishiyama, Tetrahedron Lett. 55 (2014) 3133–3146;
(d) A. Bartoszewicz, N. Ahlsten, B. Martín-Matute, Chem. Eur. J. 19 (2013) 7274–7302;
(e) R. Malacea, R. Poli, E. Manoury, Coord. Chem. Rev. 254 (2010) 729–752;
(f) C. Wang, X. Wu, J. Xiao, Chem. Asian J. 3 (2008) 1750–1770;
(g) T. Ikariya, A.J. Blacker, Acc. Chem. Res. 40 (2007) 1300–1308;
(h) X.F. Wu, J.L. Xiao, Chem. Commun. (2007) 2449–2466;
(i) J.S.M. Samec, J.-E. Bäckvall, P.G. Andersson, P. Brandt, Chem. Soc. Rev. 35 (2006) 237–248;
(j) S. Gladiali, E. Alberico, Chem. Soc. Rev. 35 (2006) 226–236;
(k) R. Noyori, S. Hashiguchi, Acc. Chem. Res. 30 (1997) 97–102.
[2] (a) D. Wang, D. Astruc, Chem. Rev. 115 (2015) 6621–6686;
(b) F. Foubelo, C. Nájera, M. Yus, Tetrahedron: Asymmetry 156 (2015) 769–790;
(c) B. Štefane, F. Požgan, Cat. Rev. - Sci. Eng. 56 (2014) 82–174;
(d) M. Darwish, M. Vills, Cat. Sci. Technol. 2 (2012) 243–255.
[3] (a) D. Carmona, F.J. Lahoz, P. García-Orduña, L.A. Oro, M.P. Lamata, F. Viguri, Organometallics 31 (2012) 3333–3345;
(b) D. Carmona, M.P. Lamata, F. Viguri, I. Dobrinovich, F.J. Lahoz, L.A. Oro, Adv. Synth. Catal. 344 (2002) 499–502;
(c) J.W. Faller, A.R. Lavoie, Organometallics 21 (2002) 3493–3495;
(d) J.W. Faller, A.R. Lavoie, Org. Lett. 3 (2001) 3703–3706.
[4] (a) G. Chelucci, S. Baldino, W. Baratta, Acc. Chem. Res. 48 (2015) 363–379;
(b) G. Chelucci, S. Baldino, W. Baratta, Coord. Chem. Rev. 300 (2015) 29–85.
[5] (*S*,*R*) and (*R*,*S*)-Josiphos = 1-[diphenylphosphano)-2-[1-(dicyclohexylphosphano) ethyl]ferrocene; (*S*,*R*) and (*R*,*S*)-Josiphos* = 1-[di(4-MeO-3,5-$Me_2C_6H_2$)phosphano)-2-[1-(dicyclohexylphosphano)ethyl]ferrocene.
[6] W. Baratta, M. Ballico, A. Del Zotto, K. Siega, S. Magnolia, P. Rigo, Chem. Eur. J. 14 (2008) 2557–2563.
[7] W. Baratta, G. Chelucci, E. Herdtweck, S. Magnolia, K. Siega, P. Rigo, Angew. Chem. Int. Ed. 46 (2007) 7651–7654.
[8] W. Baratta, G. Chelucci, S. Magnolia, K. Siega, P. Rigo, Chem. Eur. J. 15 (2009) 726–732.
[9] W. Baratta, M. Ballico, G. Chelucci, K. Siega, P. Rigo, Angew. Chem. Int. Ed. 47 (2008) 4362–4365.
[10] W. Baratta, F. Benedetti, A. Del Zotto, L. Fanfoni, F. Felluga, S. Magnolia, E. Putignano, P. Rigo, Organometallics 29 (2010) 3563–3570.
[11] W. Baratta, M. Ballico, S. Baldino, G. Chelucci, E. Herdtweck, K. Siega, S. Magnolia, P. Rigo, Chem. Eur. J. 14 (2008) 9148–9160.
[12] D. Cuervo, M.P. Gamasa, J. Gimeno, Chem. Eur. J. 10 (2004) 425–432.
[13] E. Vega, E. Lastra, M.P. Gamasa, Inorg. Chem. 52 (2013) 6193–6198.
[14] H. Nishiyama, K. Aoki, H. Itoh, T. Iwamura, N. Sakata, O. Kurihara, Y. Motoyama, Chem. Lett. 25 (1996) 1071–1072.
[15] V. Cadierno, M.P. Gamasa, J. Gimeno, L. Iglesias, Inorg. Chem. 38 (1999) 2874–2879.
[16] (a) M. Schmidlehner, P.-S. Kuhn, C.M. Hackl, A. Roller, W. Kandioller, B.K. Keppler, J. Organometal. Chem. 772–773 (2014) 93–99;
(b) J.G. Malecki, Polyhedron 45 (2012) 15–22.
[17] T. Steiner, Angew. Chem. Int. Ed. 41 (2002) 48–76.
[18] J. Díez, J. Gimeno, I. Merino, E. Rubio, F.J. Suárez, Inorg. Chem. 50 (2011) 4868–4881.
[19] (a) E. Menéndez-Pedregal, Á. Manteca, J. Sánchez, J. Díez, M.P. Gamasa, E. Lastra, Eur. J. Inorg. Chem. (2015) 1424–1432;
(b) K.J.H. Young, K.S. Lokare, C.H. Leung, M.-J. Cheng, R.J. Nielsen, N.A. Petasis, W.A. Goddard III, R.A. Periana, J. Mol. Catal. A: Chem. 339 (2011) 17–23.
[20] (a) M.M. Vinogradov, L.S. Shul'pina, Y.N. Kozlov, A.R. Kudinov, N.S. Ikonnikov, G.B. Shul'pin, J. Organomet. Chem. 784 (2015) 52–61;
(b) A.L. Müller, H. Wadepohl, L.H. Gade, Organometallics 34 (2015) 2810–2818.
[21] In a typical experiment, the ruthenium catalyst precursor (0.2 mol %) was added to a solution of acetophenone (5 mmol) in 46 mL of 2-propanol under an argon atmosphere and the mixture stirred for 15 minutes at 82 ºC. Then 0.24 mmol of KO^{t}Bu (4 mL, 0.06M in 2-propanol) (ketone/catalyst/ KO^{t}Bu ratio = 500:1:24) were added and the resulting mixture stirred for 4 h and monitored by gas chromatography.
[22] It was ascertained that this previous treatment is required and that the reaction time and temperature were optimized.
[23] When a 0.6 mol% of catalyst (ketone/catalyst/KO^{t}Bu ratio = 250:1.5:30) was employed similar conversion but slightly lower e.e. was observed (52 vs 57%).
[24] The mechanism thought to occur was proposed by us for the reduction of ketones (ref. 12) and imines (see ref. 25) catalyzed by ruthenium-pybox complexes. The role of the base is crucial as it participates in extracting the halogen and formation of the key metal-hydride species.
[25] E. de Julián, E. Menéndez-Pedregal, M. Claros, M. Vaquero, J. Díez, E. Lastra, P. Gamasa, A. Pizzano, Org. Chem. Front. 5 (2018) 841–849.
[26] (a) See representative examples: S. Enthaler, B. Hagemann, S. Bhor, G. Anilkumar, M.K. Tse, B. Bitterlich, K. Junge, G. Erre, M. Beller, Adv. Synth. Catal. 349 (2007) 853–860;
(b) J. Ito, S. Ujiie, H. Nishiyama, Chem. Commun. (2008) 1923–1925.
[27] P. Pattanayak, D. Patra, J.L. Pratihar, A. Burrows, M.F. Mahon, S. Chattopadhyay, J. Chem. Sci. 125 (2013) 51–62.
[28] (a) H. Nishiyama, Y. Itoh, Y. Sugawara, H. Matsumoto, K. Aoki, K. Itoh, Bull. Chem. Soc. Jpn. 68 (1995) 1247–1262;
(b) H. Nishiyama, Y. Itoh, H. Matsumoto, S.-B. Park, K. Itoh, J. Am. Chem. Soc. 116 (1994) 2223–2224.
[29] X. Hua, M. Shang, G. Lappin, Inorg. Chem. 36 (1997) 3735–3740. The complex *trans*-[$RuCl_2$(py){(*S*,*S*)-^{i}Pr-pybox}] was previously synthesized by reaction of [$RuCl_2$(py)(η^6-*p*-cymene)] and (*S*,*S*)-^{i}Pr-pybox in refluxing dichloromethane:.
[30] $APEX_2$ and SAINT, Bruker AXS Inc., Madison, Wisconsin, USA, 2007.
[31] G.M. Sheldrick, SADABS, University of Göttingen, Germany, 1996.
[32] CrysAlis^{Pro} CCD, CrysAlis^{Pro} RED, Oxford Diffraction Ltd., Abingdon, Oxfordshire, UK, 2008.
[33] L.J. Farrugia, J. Appl. Crystallogr. 45 (2012) 849–854.
[34] P.T. Beurskens, G. Beurskens, R. de Gelder, J.M.M. Smits, S. García-Granda, R.O. Gould, C. Smykalla, *The DIRDIF Program System*; Technical Report of the Crystallographic Laboratory, University of Nijmegen, Nijmegen, The Netherlands, 2008.
[35] A. Altomare, G. Cascarano, C. Giacovazzo, A. Guagliardi, M.C. Burla, G. Polidori, M. Camalli, J. Appl. Crystallogr. 27 (1994) 435–436.
[36] G.M. Sheldrick, SHELXL2013: Program for the Refinement of Crystal Structures, University of Göttingen, Göttingen, Germany, 2014.
[37] International Tables for X-Ray Crystallography; Vol. IV, Kynoch Press, Birminghan, U.K, 1974 present distributor Kluwer Academic Publishers: Dordrecht, The Netherlands.
[38] A.L. Spek, PLATON: A Multipurpose Crystallographic Tool, University of Utrecht, Utrecht, The Netherlands, 2016.
[39] M. Nardelli, PARST Comput. Chem. 7 (1983) 95–98.